

A Study on Yaw-Misalignment: Combined Optimization of Wind Farm Power Production and Structural Loading

Mike T. van Dijk

Master of Science Thesis

A Study on Yaw-Misalignment: Combined Optimization of Wind Farm Power Production and Structural Loading

MASTER OF SCIENCE THESIS

For the degree of Master of Science in Systems and Control at Delft
University of Technology

Mike T. van Dijk

September 5, 2016

Faculty of Mechanical, Maritime and Materials Engineering (3mE) · Delft University of
Technology

The work in this thesis was supported by the TU Delft University fund



Copyright © Delft Center for Systems and Control (DCSC)
All rights reserved.

Abstract

Climate change gives incentive for the transition to sustainable energy sources such as wind energy. To make wind energy cost competitive with fossil fuel sources, wind turbines are commonly placed in groups. As wind turbines extract energy from the wind, a wake occurs behind the turbine characterized by reduced a wind speed and increased turbulence. This wake causes down stream turbines to incur decreased power production and increased loading. Due to this aerodynamic interaction between these turbines, the energy production is sub-optimal. A control strategy to mitigate these losses is by imposing yaw misalignment with the incoming wind flow. This induces a lateral force which will cause the wake to deflect, with the goal to avoid downstream turbines. A side effect of wake deflection is partial wake overlap which has the potential to increase the fatigue loading of wind turbines. One way to decrease the cost of energy, is to increase the power production without significantly affecting the loads. Therefore, this thesis aims to quantify the load variations due to partial wake overlap and evaluate the benefits of a combined optimization of power and loads over traditional control strategies. For this purpose, we design a computational framework which computes the wind farm power production and the wind turbine rotor loads based on the yaw settings. To investigate the influence of partial wake overlap on the rotor fatigue, the differential flapwise and edgewise bending moments at hub height are computed. FLORIS is used to compute the power and CCBlade to determine the loads, supplemented with an algorithm to find the velocity distributions as hub height. The optimal yaw settings are found using a gradient-based optimization algorithm. The simulation results show that partial wake overlap can significantly increase asymmetric loading of the rotor and that yaw misalignment is beneficial in situations where the wake can be sufficiently directed away from the downstream turbines. Furthermore, a combined optimization of power and loads in all wind directions has been found to increase the average power production by 1.53% and decrease the average differential flapwise and edgewise loads by respectively 42.67% and 45.70% compared to greedy control settings. Although results are promising,

further improvements are required to confirm that mixed-objective optimization of power and loads is beneficial. We recommend the use of dynamic models to allow for more accurate load computations, validation of the results using high-fidelity models and investigating the influence of turbulence and Individual Pitch Control.

Contents

Acknowledgements	ix
1 Introduction	1
1-1 Motivation	1
1-2 Objective	2
1-3 Outline	3
2 An Introduction to Wind Farm Control	5
2-1 Axial Induction Control	5
2-2 Wake Deflection through Yaw-Misalignment and Loading	7
2-3 Other	9
2-4 Discussion	9
3 The Computational Framework	11
3-1 FLORIS*	13
3-1-1 FLORIS	13
3-2 Computation of the Optimal Rotor Velocities	17
3-3 CCBlade*	19
3-3-1 CCBlade	19
3-3-2 Computation of the Differential Loads	20
3-4 Optimizer	21
3-4-1 Optimization Problem	21
3-4-2 Game-theoretic optimization	22
3-4-3 Gradient-based optimization	23

4	Simulation results	25
4-1	The Effect of Partial Wake Overlap on Power Production and Loads	25
4-2	Optimization of the Power and the Loads for a 2-turbine case	26
4-3	Optimization of the Power and the Loads for a wind farm	28
5	Conclusion, Discussion and Recommendations	35
5-1	Conclusion and Discussion	35
5-2	Recommendations	36
	Bibliography	39
	Glossary	45
	List of Acronyms	45
	List of Symbols	45

List of Figures

2-1	An arbitrary array of wind turbines aligned in the prevailing wind direction Gebraad et al. [2014b]	6
2-2	Example of reducing the wake overlap with turbine 2 (T_2) turbine using yaw misalignment of turbine 1 (T_1) Jiménez et al. [2010]	8
2-3	A patented solution to increase the wake recovery behind a wind turbine Quek [2012]	10
3-1	Schematic of the optimization framework. The optimizer uses the power and load measurements obtained from the model to optimize the yaw settings of the wind farm. The shorthand notation $\{\zeta_i\}$ is used to indicate that $\{\zeta_i i \in \mathcal{U}\}$ where ζ_i corresponds to a property of wind turbine i and $\mathcal{U} = \{1, 2, \dots, N\}$ is the set of indices that number all turbines in a wind farm.	12
3-2	A schematic overview of a wake deflected by yaw misalignment, as modeled by FLORIS. The different wake zones are indicated.	13
3-3	Velocity distribution $\tilde{U}_{j,i}(r)$ at hub height of a wind turbine i with radius R , partially overlapped by the wake of turbine j	15
3-4	An example of a smooth gaussian distribution, fitted to a discrete velocity distribution. The curve-fitted parameters (Equation 3-2) are approximately: $\mu = 0$, $\sigma^2 = 150$, $C_s = 500$ and $U_\infty = 8$ m/s.	16
3-5	An example of a wake combination of two discrete velocity distributions on a downstream turbine	17
3-6	An example of a C_p table for a variable-pitch wind turbine Bianchi et al. [2006]	18
3-7	An example of the forces on a radial blade element s Bianchi et al. [2006]	19
4-1	Lay-out consisting of 2 turbines with an incoming wind velocity of $U_\infty = 8$ m/s. Turbine 2 is swept through the wake of turbine 1	26

4-2	The total power production (P), differential flapwise moment (ΔM_f) and edgewise moment (ΔM_e) of turbine 2 versus dY	27
4-3	Pareto fronts of total power and cumulative differential loading for various wind directions	30
4-4	Single-objective optimization of the power ($\lambda = 1.0$) for $\Phi = 0^\circ$. As a reference, the baseline power is $\sum_{i=1}^9 P_i = 8.92$ MW, and the mean differential flapwise and edgewise moments are respectively 168.03 kNm and 43.67 kNm	31
4-5	Multi-objective optimization of power and loads ($\lambda = 0.8$) for $\Phi = 0^\circ$. As a reference, the baseline power is $\sum_{i=1}^9 P_i = 8.92$ MW, and the mean differential flapwise and edgewise moments are respectively 168.03 kNm and 43.67 kNm.	32
4-6	Simulation results for the full spectrum of wind directions. All results are expressed as part of the baseline.	33
4-7	Comparison of respectively the mean total wind farm power P , mean differential flapwise ΔM_f and edgewise ΔM_e loading for all wind directions Φ . The maximum and minimum turbine loading for any wind direction that occurred in the wind farm are indicated. The tuning parameter 'C' is used analogous to λ	34

List of Tables

4-1	Optimization results for various cost functions and wind directions of a 2-turbine array. The results are expressed in % change compared to the baseline case	29
4-2	Resulting yaw settings of the various optimizations	29
4-3	Comparison of respectively the mean total wind farm power P , mean differential flapwise ΔM_f and edgewise ΔM_e loading for all wind directions Φ . Results are expressed in % change to the baseline.	34

Acknowledgements

This work in this thesis was completed at the Technical University of Delft (TUD) under supervision of dr. Jan-Willem van Wingerden and the University of Texas at Dallas (UTD) under the supervision of dr. Yaoyu Li and dr. Turaj Ashuri. First of all, I would like to thank dr. Li for providing me with all the resources required to complete this work and allowing me to attend and present at his weekly group meetings. Furthermore, I'm very grateful for dr. Ashuri's contributions to this work. He would make time to answer my questions at any time of the day, provided me with useful insights, revised my papers on Saturday nights and coached me through my 6 months at UTD. Also, I truly enjoyed our discussions about Dutch and American culture and other non-work related topics.

Another big contributor is dr. Jan-Willem van Wingerden. He made this whole experience possible by providing me with the opportunity to complete my thesis at UTD. Also, this thesis wouldn't have had the same quality without his useful ideas and inputs.

The most stressful part of moving abroad are the first few weeks. Fortunately, my lab-mate and friend Yan Xiao helped me out the first week by driving me around where ever I needed to go. On top of that, he also helped me find a place to stay, buy a phone and consulted me in the purchase of my first car.

Last but not least, I would like to thank my mother Yvonne. Throughout my studies, she has been a constant pillar of support and source of inspiration. While I was abroad, she took care of any administrative business back at home and provided me with the resources to make the best out of this experience. Also, I truly enjoyed our road trip through Texas when she visited me.

Overall this has been a very fruitful seven months. In this limited time frame, I made two publications, bought my first car, improved my English, made many new friends, have visited 8 states and have finalized my MSc degree in Control Engineering. This wouldn't have been possible without these people and for that I'm grateful.

Chapter 1

Introduction

1-1 Motivation

The increasing demand for energy is polluting the atmosphere with carbon dioxide and other global warming emissions. Among many factors that contribute to global warming, the burning of coal, natural gas and oil for electricity and heat is the largest single source Edenhofer et al. [2014]. This gives incentive for a transition to sustainable energy sources such as wind energy, which is plentiful, reliable, renewable, widely distributed and produces no greenhouse gas emissions during operation Fthenakis and Kim [2009], Denny [2009], Lewis [2007], Sims et al. [2003], Sullivan et al. [2015], Ashuri et al. [2013].

To stimulate the global rate of implementation of wind energy, it is important that wind energy is cost competitive with other energy sources. Data shows that research and innovation have greatly increased the affordability of wind energy over the past three decades Lantz et al. [2012]. Yet, the cost of wind generated electricity is generally higher than that of traditional energy resources such as coal Bolinger and Wiser [2009]. This incites continued development of the design and operation of wind turbines with the objective of reducing the cost of energy Ashuri et al. [2016b], Blanco [2009], Ashuri et al. [2016a], Spinato et al. [2009], Ashuri et al. [2014], Echavarria et al. [2008], Ashuri and Zaaier [2007], Jamieson [2011], Van Wingerden et al. [2008].

Wind turbines are generally clustered to save space and to reduce the costs associated with maintenance and cabling. A disadvantage of this setup is the aerodynamic interaction between the turbines that negatively affects the total electrical power production and the loads on the wind turbines Bianchi et al. [2006], Corten and Schaak [2003], Leithead et al. [1991]. As wind turbines extract energy from the free stream air flow, a speed deficit occurs in its wake. Any subsequent turbine in this turbulent wake will therefore

experience reduced power production. Hence, the control parameters of upstream turbines are coupled with the power production and loads of downstream turbines. The significance of such coupling manifests for smaller turbine spacing, as the wake has less time to recover. The power loss due to this phenomenon can be in the order of 10%, but is dependent on layout and atmospheric conditions Schepers and Van der Pijl [2007].

One way of mitigating these power losses is by the use of supervisory control strategies. Traditionally for below-rated wind speeds, each wind turbine aims to maximize its individual power production. This strategy is often referred to as *greedy*. It has been shown that this causes sub-optimal wind farm power production Steinbuch et al. [1988]. By taking into account the aerodynamic interaction between the turbines, it is possible to mitigate these losses Fleming et al. [2015a]. A innovative control strategy is to redirect the wake of upstream turbines away from downstream turbines using yaw-misalignment. Besides enhancing energy capture, this might result in partial wake overlap of downstream rotor blades. Therefore, yaw misalignment has the potential to influence the loads of the turbines in a wind farm Kanev and Savenije [2016].

One of the ways to decrease the cost of energy, is to increase the power production of a wind farm without significantly affecting the loads. In this thesis, we aim to achieve this by increasing the performance of a wind plant without compromising the loading due to the applied control strategies.

1-2 Objective

In this thesis, we aim to gain more insight into the phenomenon of asymmetric loading of the rotor blade due to partial wake overlap. Also, we investigate how the loading due to partial wake overlap can be included in the search for optimal yaw settings that improve the power production. To tackle this subject in an organized manner, we identify three separate research objectives that will help achieve these goals:

1. Objective 1: Quantify the significance of asymmetric loading of the rotor that is caused by partial wake overlap.
2. Objective 2: Analyze the potential of the mitigation of loading due to partial wake overlap for yaw-misalignment control strategies, which aim to increase the power production of a wind farm. The leverage of the wind direction is taken into account.
3. Objective 3: Perform an optimization of power for a wind farm without compromising the fatigue loads. This mixed-objective optimization is performed in all wind directions to establish the benefits of such a strategy over traditional optimization approaches.

These objectives will provide guidance in establishing whether a control strategy that includes both power production and fatigue loading due to partial wake overlap is beneficial over traditional strategies.

To achieve the objectives, a computational framework is created to study the effect of wakes on the power production and loading. The considered loads are the differential flap and edgewise moments. The framework consists of a model to describe the steady-state wake properties on a wind farm level and a model to compute the power production and loading at each wind turbine. The optimal yaw angles for all turbines are found using an optimizer.

1-3 Outline

To efficiently answer the research objectives, this thesis is divided into 5 chapters. The outline is as follows:

1. Chapter 2: An introduction to the most prominent wind farm control methods is given. The reader is informed about the state-of-the-art and each method is briefly discussed.
2. Chapter 3: In this chapter, we introduce the computational framework that is essential for obtaining the results. The framework is split into several sub-models, each explained individually.
3. Chapter 4: Here, the results are presented of 3 simulation studies. The first results quantify the load variations due to partial wake overlap. Furthermore, optimization results are presented of a 2-turbine setup and a wind farm.
4. Chapter 5: The work is concluded and recommendations are given for future work.

Chapter 2

An Introduction to Wind Farm Control

Reduced wind farm power production due to aerodynamic interaction between the turbines can be mitigated by changing the lay-out and by using wind farm control techniques. Generally wind turbine controllers are set to maximize their individual power production while mitigating loads. This control strategy is also referred to as *greedy*. It has been suggested that higher level wind farm supervisory control is advantageous over this strategy, as this takes into account the total power production Steinbuch et al. [1988], Spruce [1993]. In this chapter, two popular control strategies are explained: *Axial induction control* and *yaw-misalignment*. Furthermore, insight is given into possible loading issues as a result of yaw-misalignment.

2-1 Axial Induction Control

One control strategy to mitigate the energy losses is axial induction control. The axial induction factor a describes the relation between the velocity of the incoming wind stream and the velocity of the wind leaving the rotor plane of the turbine Bianchi et al. [2006]. Therefore its an indicator of the amount of aerodynamic energy extracted from the wind by the turbine. Wind turbines have internal controllers that try to maximize the energy capture P at below rated wind conditions by changing the pitch of the blades and the torque of the generator. In Figure 2-1 an array of wind turbines is displayed, with axial induction factors as inputs and power as outputs. By decreasing the axial induction factor of an upstream turbine, the velocity deficit in the wake will decrease and subsequent turbines will experience increased power production. This method has the potential to increase the total power production of the wind farm Annoni et al. [2015].

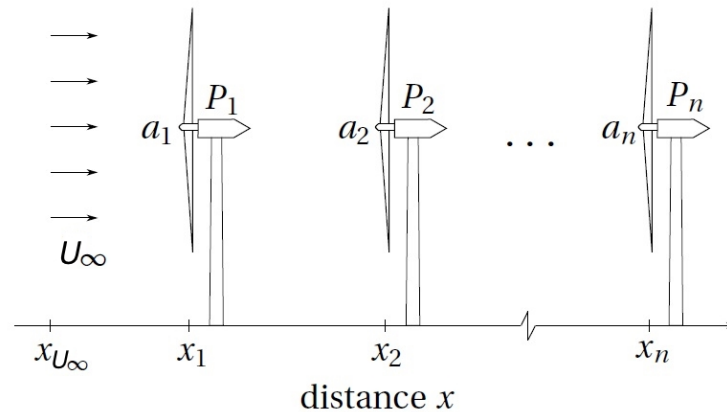


Figure 2-1: An arbitrary array of wind turbines aligned in the prevailing wind direction [Gebraad et al. [2014b]]

Various authors have done research on the benefits of axial induction control, primarily using simulation tools. The majority of the authors used a model-based approach. Heer et al. [2014] maximized the wind farm energy output by designing a MPC controller using the Jensen wake model Jensen [1983]. An increase in power production of 1% was reported, but with a side-note that the gain greatly depends on the wake model used. Authors like Herp et al. [2015] and Behnood et al. [2014] solved the problem using a model similar to the Jensen model. Herp et al. [2015] used a sequential optimization in a model-based approach and produced mixed results. Specifically, the power gain appeared to rely heavily on the wake expansion parameter which has a negative effect on the potential gain of the power optimization. Behnood et al. [2014] used a particle swarm optimization and found a total energy increase of 1.86% for a 4x4 turbine wind farm. Horvat et al. [2012] also used a sequential programming function in Matlab, but used a static engineering model published by Brand [2009]. They reported a power gain of 2.85% at lower wind speeds. At higher wind speeds, the goal was to optimize the wind farm loads. They showed that the loads in the wind farm can be equalized among all turbines by axial induction control. Serrano Gonzalez et al. [2013] used a genetic algorithm in combination with a static wake model by Frandsen et al. [2006] to optimize a row of wind turbines. They performed a sensitivity analysis of the spacing between turbines on the potential power gain by a wind farm controller. It was found that the rate of improvement declined as the distance between turbines increased. The authors chose for a distance of six times the rotor diameter for their simulation, but did not provide a clear motivation.

While the previously mentioned authors focused on using engineering models, Goit and Meyers [2015] used a high fidelity simulation to obtain data on the wake interaction between turbines. They optimized the total energy output using a conjugate gradient optimization. They found that the increases in energy extraction for a row of 6 turbines

is in the order of 6%, for a simulation time of one hour.

Other authors focused on model-free approaches with the benefit that no knowledge of the aerodynamic interaction between turbines is required. For instance, Marden et al. [2013] proposed a game-theoretic approach. They showed that under stationary atmospheric conditions, it is possible to optimize the power without the use of a model. Two simplistic wind farm examples were simulated, and efficiency gains in upwards of 25% were observed compared to the greedy algorithm. Gebraad et al. [2013] implemented a gradient-based optimization algorithm in a distributed control setting for a row of wind turbines, and later for a wind farm [Gebraad and van Wingerden, 2015]. In the latter, it was shown that the presented algorithm converged faster than the game-theoretic optimization. A similar gradient-descent algorithm was used by Kim et al. [2014] in a model-free approach. They decreased the convergence time of the algorithm by implementing a variable-step size according to wind conditions. Yang et al. [2013] optimized the power of a row of wind turbines using extremum seeking control. Here the turbines are optimized in a nested-loop framework, from downstream to upstream units in a sequential manner. This results in a power gain of 9.09% for a row of three turbines. Their simulation results suggested that the optimal control settings are invariant with the wind speed. Rotea [2014] has shown that wind farm power optimization problems may be solved with dynamic programming, which reduces the complexity of the optimization and provides a formal mechanism for computing limits of performance in wind farms, as well as rigorous proof that the nested loop extremum seeking control approach advanced in Santoni et al. [2015] is optimal. A Bayesian optimization algorithm was implemented with a modified sampling procedure by Park and Law [2015]. Bayesian optimization builds a model using a gaussian process which is utilized to find new inputs that yields improvement of the total power production. The authors implemented the algorithm on an experimental setup of two turbines in a wind tunnel. Results showed that, although the algorithm was not able to reach the global optimum, it significantly improved the wind turbine power by executing only a small number of control actions. Corten and Schaak [2003] performed a wind tunnel experiment of three rows of 8 scaled turbines and concluded that the power extraction could be increased by derating the upstream turbines.

2-2 Wake Deflection through Yaw-Misalignment and Loading

A more innovative technique is to redirect the wake away from downstream turbines by creating yaw misalignment of the turbine with the incoming wind Knudsen et al. [2014]. Although yawing a turbine decreases its power production, the wake deflection can reduce the wake overlap with the downstream turbine (Figure 2-2). As the downstream turbine will experience a higher effective wind velocity, it will generate more power.

A few sources have performed both simulation and experimental studies, to investigate the benefits of yaw-misalignment. Gebraad et al. [2014b] designed and used a model

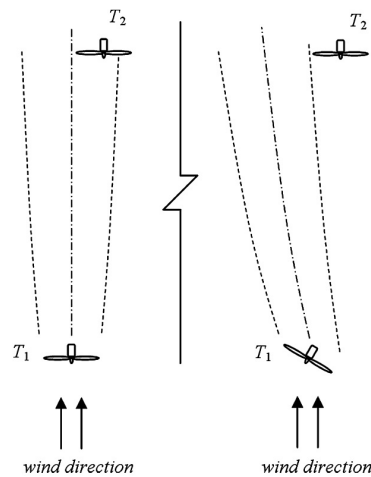


Figure 2-2: Example of reducing the wake overlap with turbine 2 (T_2) turbine using yaw misalignment of turbine 1 (T_1) Jiménez et al. [2010]

to perform a power optimization using a game theoretic algorithm and validated the results with a high-fidelity simulation. A power increase of 13% was observed with respect to the greedy case. Fleming et al. [2015b] optimized both the layout and the power production of the wind farm using a steady-state model to describe the wake properties and a sequential quadratic programming method. It was found that the best overall improvement was achieved by the coupled control and position optimizations. Schottler et al. [2016] found through a wind tunnel test of two scaled turbines that the power production of the downstream turbine was coupled with the yaw of the upstream turbine. They suggested that yawing the upstream turbine can increase the total power production. Park and Law [2015] implemented the bayesian ascent algorithm on an array of two turbines in a wind tunnel, where they optimized both the yaw and the axial induction factors. The algorithm suffered from measurement noise, but was nonetheless able to increase the total power generated by the two wind turbines.

Various results have been reported on wind turbine loading due to yaw misalignment. Boorsma [2012], Ashuri and Zaaijer [2008] and Capponi et al. [2011] found that the blade edgewise moments are mainly dominated by gravity forces and are not heavily coupled with yaw-misalignment. Similar results were found by Fleming et al. [2015a] using SOWFA Fleming et al. [2013]. They also discovered an increase in out-of-plane bending moments, drivetrain torsion and tower-base bending moments of the downstream turbine. These loads are likely caused by the transition from full to partial wake overlap and turbulence in the wake. Kragh and Hansen [2014] suggested that the blade out-of-plane bending moments of upstream turbines decrease by a yaw-misalignment in the range of -10° to 30° . Churchfield et al. [2015] showed an increase in the blade out-of-plane bending moments of downstream turbines due to yaw misalignment. This shows that while upstream turbines generally benefit, downstream turbines can experience increased loads. Finally, Eggers et al. [2003] found that wind shear significantly increased

the rotor fatigue loads. Extending this to horizontal wind shear suggests partial wake overlap can similarly influence the fatigue loads.

Limited research has been done on rotor loading due to partial wake overlap. When a wake is deflected, the downstream turbine might experience partial wake overlap. As the velocity of the incoming wind flow can be much lower on the side of the rotor blade that overlaps with the wake, it will experience asymmetric loading. This has the potential to increase the fatigue loads of the turbine. This was shown by Kanev and Savenije [2016], whom found that partial wake overlap increased the Damage Equivalent Loads (DEL) by 15-20% when the wake center would be at the edge of the rotor. Note that the magnitude of the increase in DEL depends on many factors such as turbine spacing, wind direction and other atmospheric properties.

2-3 Other

Besides yaw-misalignment, other ideas exist on how to redirect the wake. One method would be to tilt the rotor, to redirect the wake towards the ground. Unfortunately, modern day turbines at the time of writing are not designed to allow rotor tilting. This could be solved by the use of individual pitch control to tilt the rotor. But this comes with the disadvantage of significantly increasing the structural loads Fleming et al. [2014].

Furthermore, a number of experimental solutions have been patented, but no records of these being built exist at the time of writing Quek [2012]. These solutions focus on increasing the wake recovery. One of the solutions describes a device at the front of the turbine drawing in air and expelling the accelerated stream, in the form of a vortex flow, at the rear of the turbine (Figure 2-3). Another solution proposes curved rotor blades with the aim to create a vortex in the wake such that it recovers faster. Finally, Churchfield et al. [2014] suggested to relocate the turbines for floating wind farms such that the wakes of upstream turbines are evaded.

2-4 Discussion

Not all the methods discussed beforehand are equally suitable to mitigate the power losses due to aerodynamic interaction within a wind farm. Most positive results for axial induction control are obtained under stationary atmospheric conditions and using simplified models. As these studies present small potential gains in power production, one can question the effectiveness of axial induction control on a real wind farm. A lack of experimental research further feeds this uncertainty.

Studies on yaw-misalignment have presented some promising results on the wind farm power production. Unfortunately, this control method is relatively new and therefore

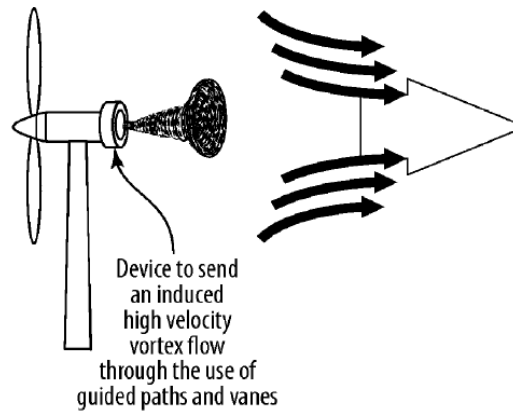


Figure 2-3: A patented solution to increase the wake recovery behind a wind turbine Quek [2012]

hasn't been investigated to the full potential yet. Similar to axial induction control, full-scale experimental studies lack so the effectiveness can't be verified. The research done on the structural loading due to yaw misalignment mostly reports load reduction, but fails to address the topic of partial wake overlap. Therefore, more research is required to verify the applicability of this method.

The remaining methods all have obvious disadvantages to them or are impossible to implement on the modern generation of wind turbines. Therefore, yaw-misalignment is the most promising control method to mitigate the power losses in a wind farm but requires further research of the effects on structural loading.

The Computational Framework

A computational framework has been developed to analyze the impact of wake effects on the power production and loading. The framework consists of steady-state models which are computationally efficient, in order to limit the computational resources required for optimization. A wind farm consisting of NREL 5MW baseline turbines Jonkman et al. [2009] is used. As the use of steady-state models eliminates the possibility to use dynamic methods for load representation, the loads considered are the maximum-to-minimum difference of the flap (ΔM_f) and edgewise (ΔM_e) moments (Section 3-3) at hub height. These are chosen to capture the asymmetric load distribution on a rotor blade due to partial wake overlap. To facilitate this, an algorithm that computes the velocity distribution at the rotor disk is implemented as described in Section 3-1-1.

Figure 3-1 shows the framework that consists of a modified version of the FLOW Redirection and Induction in Steady-state (FLORIS) model Gebraad et al. [2014a], a modified version of CCBlade Ning [2013] and an optimizer¹². In the *FLORIS** module, the effective wind velocities and velocity distributions in the lateral direction at hub height at each wind turbine are calculated. The module '*Find Ω* ' determines the optimal rotor velocity for every turbine based on the effective wind velocity. The optimal rotor velocity and the velocity distribution are used to compute the power production and the loads at every turbine in the module *CCBlade**. The *Optimizer* subsection closes the loop by including the power production and the loads of the wind farm in one cost function, and is used to find the optimal yaw settings.

¹FLORIS: <https://github.com/WISDEM/FLORISSE>, accessed: 04-March-2016

²CCBlade: <https://github.com/WISDEM/CCBlade>, accessed: 04-March-2016

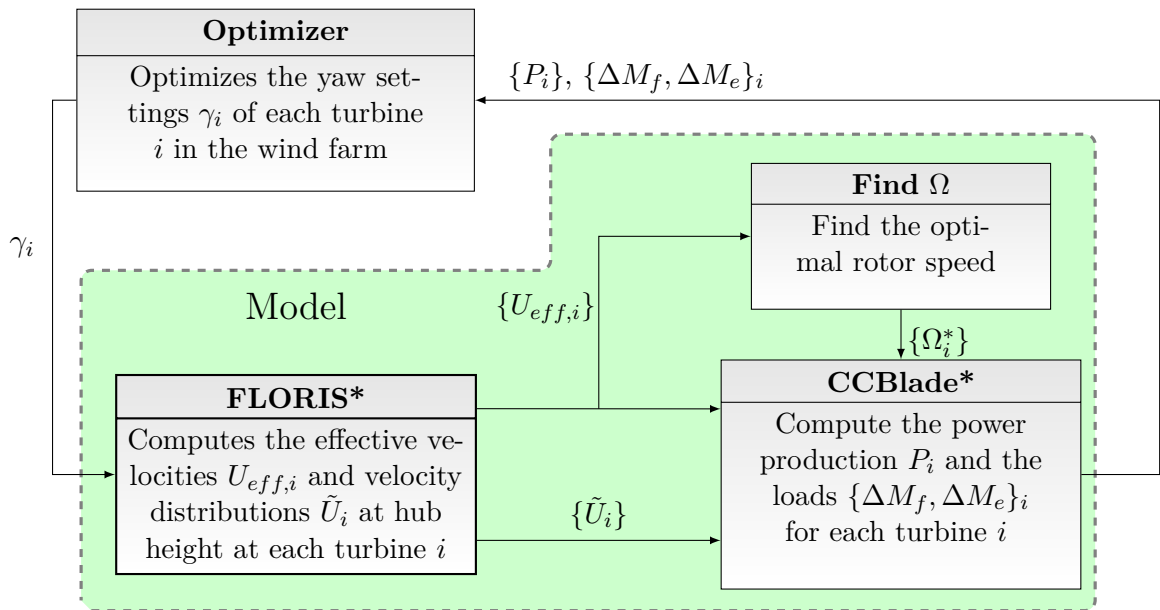


Figure 3-1: Schematic of the optimization framework. The optimizer uses the power and load measurements obtained from the model to optimize the yaw settings of the wind farm. The shorthand notation $\{\zeta_i\}$ is used to indicate that $\{\zeta_i | i \in \mathcal{U}\}$ where ζ_i corresponds to a property of wind turbine i and $\mathcal{U} = \{1, 2, \dots, N\}$ is the set of indices that number all turbines in a wind farm.

3-1 FLORIS*

FLORIS* is used to compute the effective wind velocities U_{eff} and the velocity distributions at hub height \tilde{U} of each turbine. These are respectively used for the computation of the power and the differential flapwise and edgewise loads, as will be explained in Section 3-3. FLORIS* is an extended version of FLORIS, in that it adds an algorithm to compute the velocity distributions at hub height \tilde{U} .

3-1-1 FLORIS

FLORIS is a data-driven model that describes the steady-state wake characteristics as a function of axial inductions and yaw-misalignment. It uses the velocity profiles of the wakes to compute the power of each individual turbine. The wake is modeled using an augmented version of the Jensen model Jensen [1983]. The fidelity of the model is increased by dividing the wake in three zones with individual expansion and velocity properties (Figure 3-2). Therefore, the velocity is assumed to be uniform in lateral direction within a wake. The wake deflection due to yaw-misalignment and rotational effects is characterized as in Jiménez et al. [2010].

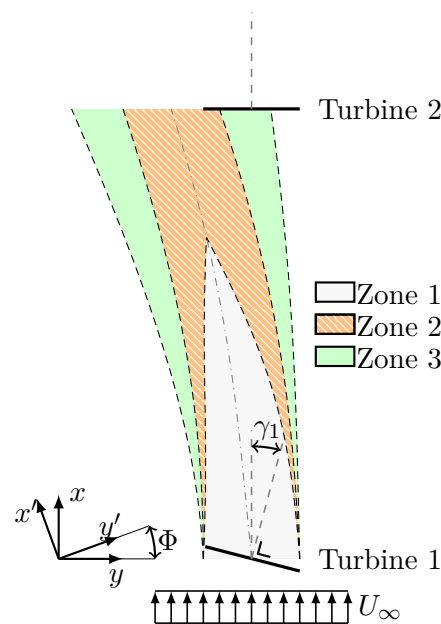


Figure 3-2: A schematic overview of a wake deflected by yaw misalignment, as modeled by FLORIS. The different wake zones are indicated.

The model contains a small amount of parameters to describe the properties of the wake and the computation of the power. These parameters can be tuned such that the power predicted by FLORIS can be fit to the time-averaged results from high-fidelity simulation

data of wind farms. The benefit of FLORIS is that it is computationally efficient yet relatively accurate due to the identification using high-fidelity simulation data. FLORIS defines a local (x, y) , and a global (x', y') coordinate system to accommodate for different wind directions Φ (Figure 3-2). The yaw γ_i of a turbine i is used to compute its wake deflection. For a wake caused by turbine j , the velocity in each corresponding wakezone z at the x-coordinate of a turbine i is defined by $U_{j,i,z}$, $z \in \{1, 2, 3\}$.

FLORIS computes the effective wind velocity, $U_{eff,i}$, at a downstream turbine i by combining all the overlapping wakes at its rotor disk. This is done by weighting the wake velocities $U_{j,i,z}$ by their overlap of the corresponding wake zones with the rotor using the root-sum-square method of Katic et al. [1986]. For a detailed description of the FLORIS model, the reader is referred to Gebraad et al. [2014a].

Velocity Distribution

FLORIS* computes the velocity distributions at hub height which are used by CCBlade* to compute the differential loads. For this purpose, we introduce the set of indices $\mathcal{U} = \{1, 2, \dots, N\}$ that number all turbines in a wind farm. Each turbine $j \in \mathcal{U} \setminus \{i\}$ has a velocity distribution over turbine i denoted by $\tilde{U}_{j,i}(y_{r,i})$. We define the local y-coordinate $y_{r,i}$ on the rotor disk of turbine i at hub height as shown in Figure 3-3.

Because FLORIS assumes the velocity within a wake zone to be uniform in lateral direction, the nature of the velocity distribution \tilde{U} is discrete. This has been shown to cause local minimums in the cost function (i.e. Figure 4-2), obstructing the use of gradient-based optimization algorithms. To solve this, the discrete velocity distribution is transformed to a smooth velocity distribution with the use of a curve-fitting algorithm.

Curve-fitting

The discrete nature of the velocity distribution modeled by FLORIS causes local minimums to appear in the cost-function. In a real wake, this is also unrealistic as the velocity will gradually decrease as the center of the wake is approached. Therefore, a smooth velocity distribution is estimated based on the information of the discrete velocity distribution. Note that the problem of local minimums is no concern when global optimization algorithms are used. Therefore, smoothing the velocity distribution was only applied for the results published in Section 4-3.

We smooth out the velocity distribution by fitting a function to the discrete wake data. For this purpose, a Gaussian distribution function is chosen:

$$f_{gauss}(x) = \frac{1}{\sigma\sqrt{2\pi}} e^{-\frac{(x-\mu)^2}{2\sigma^2}} \quad (3-1)$$

The parameters μ and σ can be used to transform the shape of the function. To properly fit the Gaussian distribution function to the discrete velocity distribution, some modifications are made. The function is inverted, and some parameters to allow scaling are

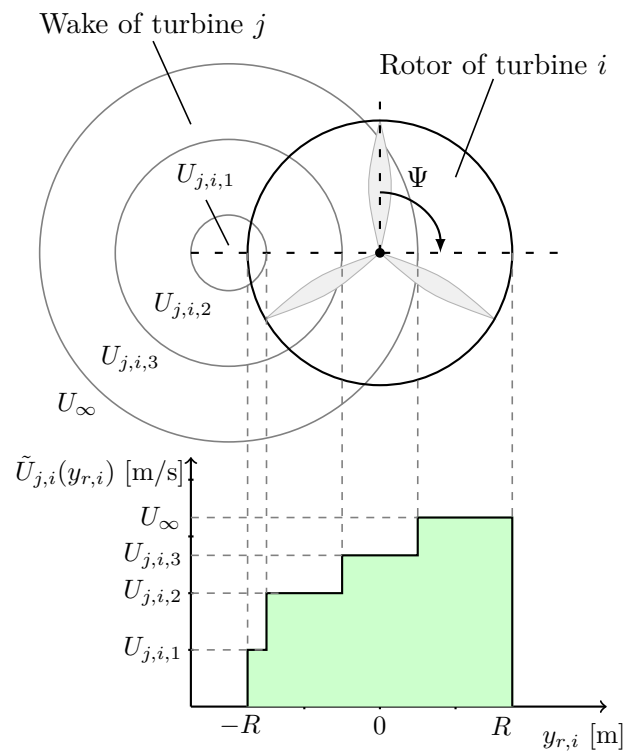


Figure 3-3: Velocity distribution $\tilde{U}_{j,i}(r)$ at hub height of a wind turbine i with radius R , partially overlapped by the wake of turbine j

added. The resulting inverted Gaussian distribution is defined as follows:

$$\tilde{U}_{fit,j,i}(y_{r,i}) = U_{\infty} - C_s \frac{1.0}{\sigma\sqrt{2\pi}} e^{-\frac{(y_{r,i}-\mu)^2}{2\sigma^2}} \quad (3-2)$$

where μ (-), σ (-), C_s (-) are parameters used for fitting and U_{∞} (m/s) is the incoming free-stream wind velocity. Note that most these parameters are dimensionless as they are only used to obtain a good fit to the discrete velocity distribution. The parameters are found using a non-linear least squares curve fitting algorithm Markwardt [2009].

A comparison is made between a discrete and Gaussian velocity profile of a wake in Figure 3-4. It can be seen that the smooth velocity distribution resembles the discrete distribution.

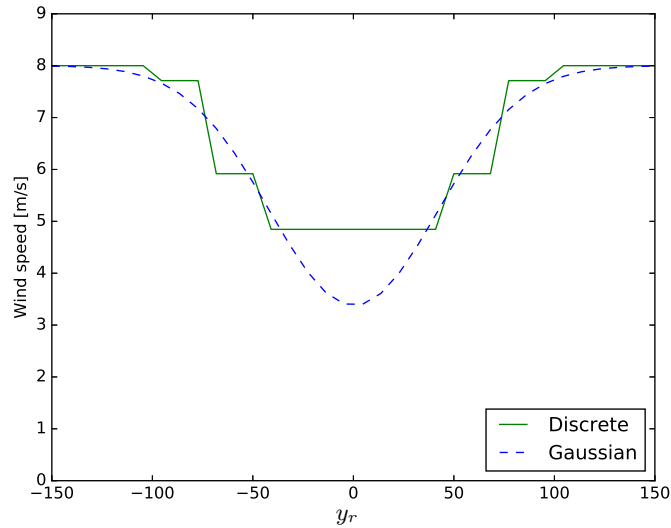


Figure 3-4: An example of a smooth gaussian distribution, fitted to a discrete velocity distribution. The curve-fitted parameters (Equation 3-2) are approximately: $\mu = 0$, $\sigma^2 = 150$, $C_s = 500$ and $U_{\infty} = 8$ m/s.

Combining wakes

When several wakes overlap the same turbine, the velocities in the wake zones have to be combined in order to obtain the velocity distribution. This is done for every turbine in the wind farm similar to FLORIS, by applying the root-sum-square method.

To limit the amount of unnecessary wake combinations that have to be computed, only the wakes of upstream turbines are taken into account. Therefore, for each turbine i the set $\mathcal{F}_i \subset \mathcal{U}|_{x_j < x_i}$ of upstream turbines j is introduced.

Now each turbine j will have a velocity distribution over downstream turbine i (i.e. Figure 3-2). To obtain the combined velocity distribution $\tilde{U}_i(y_{r,i})$, the velocities of each wake that overlaps with the rotor of turbine i with radius R have to be combined. Hence, for any $y_{r,i}$ in the range $[-R, R]$, $\tilde{U}_i(y_{r,i})$ is obtained as follows:

$$\tilde{U}_i(y_{r,i}) = \begin{cases} U_\infty \left(1 - \sqrt{\sum_{j \in \mathcal{F}} \left(1 - \frac{\tilde{U}_{fit,j,i}(y_{r,i})}{U_\infty} \right)^2} \right) & \text{for } \mathcal{F}_i \neq \emptyset, \\ U_\infty & \text{for } \mathcal{F}_i = \emptyset. \end{cases} \quad (3-3)$$

where U_∞ is the velocity of the incoming wind flow. If the turbine has no upstream turbines, the set \mathcal{F}_i will be empty and its velocity distribution will be set equal to the incoming wind speed U_∞ .

In Figure 3-5, an example is shown of the wake combination for an array of 3 turbines. The velocity distributions of the first 2 turbines over the rotor of turbine 3 ($\tilde{U}_{1,3}$, $\tilde{U}_{2,3}$) are combined (\tilde{U}_3). The rotor has a radius of $R = 63$ m.

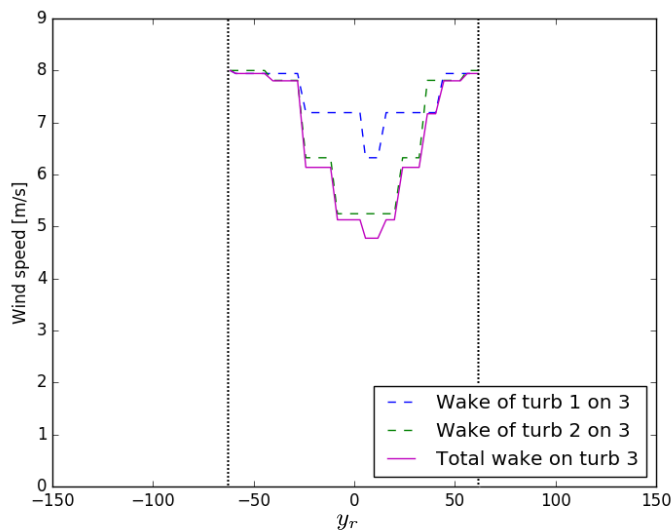


Figure 3-5: An example of a wake combination of two discrete velocity distributions on a downstream turbine

3-2 Computation of the Optimal Rotor Velocities

Each turbine is assigned a steady-state rotational speed based on the effective wind velocity U_{eff} it experiences. It is assumed that every turbine's internal controller will try to maximize its power production at below rated wind speeds Leithead et al. [1991],

Ashuri et al. [2010]. This corresponds to maximizing the power coefficient C_p . The power coefficient describes the ability of a wind turbine to capture energy and is defined as:

$$C_p = \frac{P_D}{P_V} \quad (3-5)$$

where P_D is the aerodynamic energy extracted by the rotor and P_V is the energy in the wind fed to the turbine. The power coefficient is typically modeled as a function of tip-speed-ratio λ_{tip} and blade pitch β Bianchi et al. [2006], Ashuri [2012]. An example of a typical $C_p(\lambda_{tip}, \beta)$ graph is shown in Figure 3-6. The optimal tip-speed-ratio λ_{tip}^* and blade pitch β^* that maximize the power coefficient C_p are indicated. The tip-speed-ratio

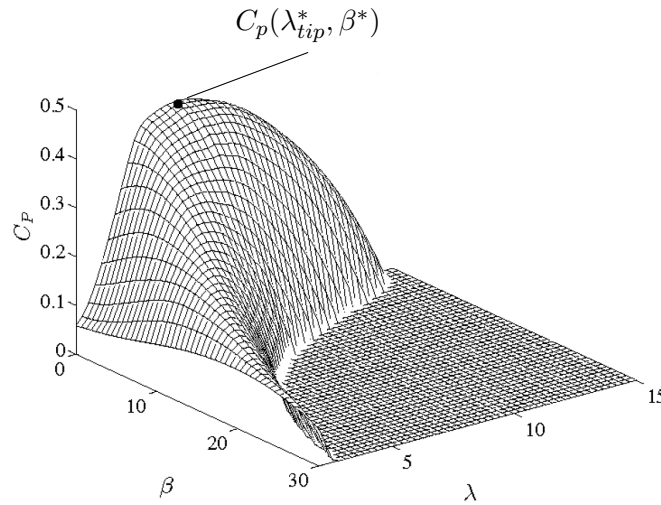


Figure 3-6: An example of a C_p table for a variable-pitch wind turbine Bianchi et al. [2006]

of turbine i is defined as:

$$\lambda_{tip,i} = \frac{R\Omega_i}{U_{eff,i}} \quad (3-6)$$

Now the blade pitch β is assumed to be 0 as the turbine operates in below-rated wind conditions, hence the power coefficient is $C_p(\lambda, 0)$. The definition of the tip-speed-ratio can be used to estimate the optimal steady-state rotor speed Ω_i^* for turbine i as follows:

$$\Omega_i^* = \frac{\lambda_{tip,i}^* U_{eff,i}}{R} \quad (3-7)$$

where $\lambda_{tip,i}^*$ is the tip-speed-ratio that maximizes the corresponding power coefficient $C_{p,i}(\lambda_i^*, 0)$ and $U_{eff,i}$ is the local effective wind velocity. The C_p -table for the NREL 5MW turbine is obtained using *WT perf* Platt and Buhl [2012] which is a simulation tool developed by NREL that uses blade-element momentum theory (Section 3-3) to predict the performance of wind turbine blades.

3-3 CCBlade*

CCBlade* is an extended version of CCBlade, in that it adds an algorithm to compute the load variations due to partial wake overlap. CCBlade is an implementation of a reliable method to solve the blade element momentum (BEM) equations Ning [2014] and predicts the aerodynamic power production and loading of wind turbine blades.

3-3-1 CCBlade

CCBlade is an implementation of the BEM equations and analyzes the aerodynamic forces on a radial blade element of infinitesimal length. The analysis is carried out by dividing the stream tube containing the rotor swept area into concentric infinitely small tubes which are each treated independently. For practical purposes, the length of each blade is divided up into S segments, where each segment is indicated by $s \in \{\frac{1}{S}R, \frac{2}{S}R, \dots, R\}$. Similarly, the rotor swept area is also divided into M angular segments along the azimuth angle indicated by $m \in \{\frac{1}{M}2\pi, \frac{2}{M}2\pi, \dots, 2\pi\}$. An example of the forces on a radial blade element can be seen in Figure 3-7. As the rotor rotates, the blade element will move at a relative speed V_{rel} in the wind flow. Therefore for a blade element s at angular segment m , V_{rel} can be computed from the effective wind velocity U_{eff} and the tangential blade element speed $r\Omega_r$:

$$V_{rel,s,m} = \sqrt{(U_{eff} * (1 - a_{s,m}))^2 + (r_s \Omega_r * (1 + a'_{s,m}))^2} \quad (3-8)$$

where $a_{s,m}$ is the axial induction factor and $a'_{s,m}$ is the tangential axial induction factor. The axial induction factors and the local flow direction $\phi_{b,m}$ are computed for each blade element s and each angular segment m using a technique described in Ning [2014]. Each blade element has its individual lift coefficient $C_{L,s}$, drag coefficient $C_{D,s}$ and cord

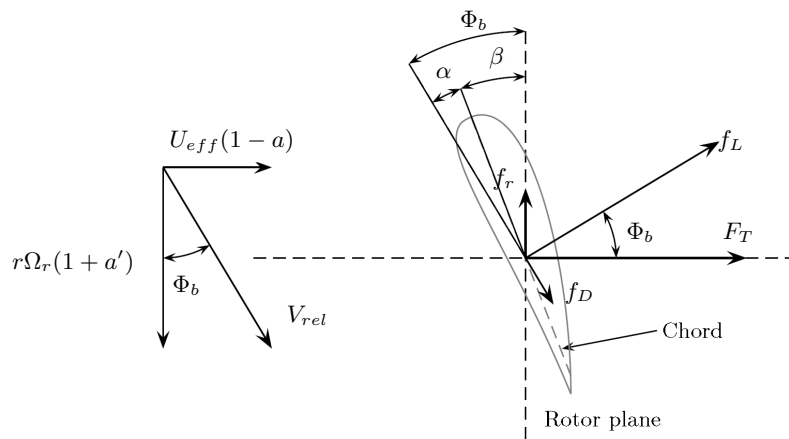


Figure 3-7: An example of the forces on a radial blade element s Bianchi et al. [2006]

length c_s . The local axial thrust force $Q_{p,s,m}$ and local torque $T_{p,s,m}$ for each segment are computed using these parameters as follows:

$$\begin{aligned} Q_{p,s,m} &= \frac{\rho c_s}{2} V_{rel,s,m}^2 (C_{L,s}(\alpha) \cos(\phi_{b,s}) + C_{D,s}(\alpha) \sin(\phi_{b,s})) \\ T_{p,s,m} &= \frac{\rho c_s}{2} V_{rel,s,m}^2 r (C_{L,s}(\alpha) \sin(\phi_{b,s}) + C_{D,s}(\alpha) \cos(\phi_{b,s})) \end{aligned} \quad (3-9)$$

where α is the incidence angle computed using the angle between the local flow direction and the rotor plane ($\phi_{b,s}$), the blade pitch angle (β) (see Ning [2014]). Now the total thrust force F_{tot} and torque Q_{tot} over one rotor rotation can be determined by integrating the local axial thrust force and torque over all blade elements and azimuth segments:

$$F_{tot} = N_b \int_0^{2\pi} \int_0^R Q_{p,s,m} ds dm, \quad Q_{tot} = N_b \int_0^{2\pi} \int_0^R T_{p,s,m} ds dm \quad (3-10)$$

where N_b represents the number of blades ($N_b = 3$). The aerodynamic power for a turbine i , assuming an optimal rotor speed, can be computed by:

$$P_i = Q_{tot,i} \Omega_i^* \quad (3-11)$$

3-3-2 Computation of the Differential Loads

The selected loads are the maximum-to-minimum differential flapwise and edgewise bending moments at hub height. Because steady-state models are utilized, it is not possible to use advanced methods for computing fatigue loads such as Rainflow-counting Downing and Socie [1982]. Furthermore, certain effects such as the transition from full to partial wake overlap, wind shear and turbulence aren't modeled. Hence, we seek a measure to describe the effect of partial wake overlap on the fatigue loads of the rotor.

To measure the loads on the rotor, the flapwise and edgewise bending moments are chosen. Throughout one full rotation of a rotor blade, the maximum and minimum bending moments resulting from partial wake overlap are expected to occur in any order at the azimuth angles $\Psi = 90^\circ$ and $\Psi = 270^\circ$. This corresponds to the bending moments when a blade is at hub height. By taking the difference in bending moments between these locations, the load variation of the rotor during one rotation is obtained. This will be used analogously to the fatigue due to partial wake overlap.

Finally, the maximum-to-minimum difference of the flap and edgewise moments are determined. To be able to detect the influence of partial wake overlap on the loading, CCBlade* is expanded to take into account a velocity distribution. The flapwise and edgewise bending moments at $\Psi = 90^\circ$ and $\Psi = 270^\circ$, are obtained using the velocity distribution $\tilde{U}_i(y_{r,i})$ at hub height (Section 3-1-1). For this purpose, $\tilde{U}_i(y_{r,i})$ is split into two distributions of S elements defined as:

$$\begin{aligned} \tilde{U}_{i,s,\Psi=90^\circ} &= \tilde{U}_i(y_{r,i}) \text{ where } y_{r,i} \in \{0, \frac{1}{S}R, \frac{2}{S}R, \dots, R\} \\ \tilde{U}_{i,s,\Psi=270^\circ} &= \tilde{U}_i(y_{r,i}) \text{ where } y_{r,i} \in \{0, -\frac{1}{S}R, -\frac{2}{S}R, \dots, -R\} \end{aligned} \quad (3-12)$$

Now the local axial thrust force $Q_{p,s,m}$ and local torque $T_{p,s,m}$ on each blade element are obtained by:

$$\begin{aligned}
Q_{p,s,\Psi=90^\circ} &= \frac{\rho c_s}{2} \tilde{U}_{i,s,\Psi=90^\circ}^2 (C_{L,s}(\alpha) \cos(\phi_{b,s}) + C_{D,s}(\alpha) \sin(\phi_{b,s})) \\
Q_{p,s,\Psi=270^\circ} &= \frac{\rho c_s}{2} \tilde{U}_{i,s,\Psi=270^\circ}^2 (C_{L,s}(\alpha) \cos(\phi_{b,s}) + C_{D,s}(\alpha) \sin(\phi_{b,s})) \\
T_{p,s,\Psi=90^\circ} &= \frac{\rho c_s}{2} \tilde{U}_{i,s,\Psi=90^\circ}^2 r (C_{L,s}(\alpha) \sin(\phi_{b,s}) + C_{D,s}(\alpha) \cos(\phi_{b,s})) \\
T_{p,s,\Psi=270^\circ} &= \frac{\rho c_s}{2} \tilde{U}_{i,s,\Psi=270^\circ}^2 r (C_{L,s}(\alpha) \sin(\phi_{b,s}) + C_{D,s}(\alpha) \cos(\phi_{b,s}))
\end{aligned} \tag{3-13}$$

These are used to obtain the flapwise and edgewise bending moments at $\Psi = 90^\circ$ and $\Psi = 270^\circ$:

$$\begin{aligned}
M_{f,\Psi=90^\circ} &= \int_0^R s Q_{p,s,\Psi=90^\circ} ds, & M_{f,\Psi=270^\circ} &= \int_0^R s Q_{p,s,\Psi=270^\circ} ds \\
M_{e,\Psi=90^\circ} &= \int_0^R T_{p,s,\Psi=90^\circ} ds, & M_{e,\Psi=270^\circ} &= \int_0^R T_{p,s,\Psi=270^\circ} ds
\end{aligned} \tag{3-14}$$

Finally, the maximum-to-minimum flapwise and edgewise bending moment differences are computed as follows:

$$\Delta M_f = |M_{f,\Psi=90^\circ} - M_{f,\Psi=270^\circ}|, \quad \Delta M_e = |M_{e,\Psi=90^\circ} - M_{e,\Psi=270^\circ}| \tag{3-15}$$

3-4 Optimizer

The optimizer will search for the yaw-settings that maximize the power and minimize the loads. For the results presented in Section 4-2 a game-theoretic optimization approach was utilized Marden et al. [2013], and for the results shown in Section 4-3 a gradient-based optimization algorithm. In the remainder of this section, the optimization problem will be formulated and these optimization approaches will be explained.

3-4-1 Optimization Problem

The goal of the optimizer is to find the set of yaw-settings $\gamma = \{\gamma_1, \gamma_2, \dots, \gamma_N\}$ that minimizes the cost function (Section 4-2). To achieve the objective, a constrained minimization problem is defined as follows:

$$\begin{aligned}
&\underset{\gamma}{\text{minimize}} && c(\gamma) \\
&\text{subject to} && |\gamma_i| \leq \gamma_{max}, i = 1, \dots, N
\end{aligned} \tag{3-16}$$

where γ_{max} is the maximum allowable yaw angle and is chosen to be $\gamma_{max} = 40^\circ$. This constraint is added to limit the search space. The cost functional $c(\gamma)$ combines the

power and the loads of a turbine $i \in \mathcal{U}$ as follows:

$$c(\boldsymbol{\gamma}) = -\lambda \underbrace{\left(\sum_{i=1}^N \bar{P}_i(\boldsymbol{\gamma}) \right)}_{\text{power}} + \frac{(1-\lambda)}{2N} \underbrace{\left(\sum_{i=1}^N \Delta \bar{M}_{f,i}(\boldsymbol{\gamma}) + \sum_{i=1}^N \Delta \bar{M}_{e,i}(\boldsymbol{\gamma}) \right)}_{\text{loads}} \quad (3-17)$$

$$\bar{P}_i(\boldsymbol{\gamma}) = \frac{P_i(\boldsymbol{\gamma})}{\tilde{P}_{max}}, \quad \Delta \bar{M}_{f,i}(\boldsymbol{\gamma}) = \frac{\Delta M_{f,i}(\boldsymbol{\gamma})}{\Delta \tilde{M}_{f,max}}, \quad \Delta \bar{M}_{e,i}(\boldsymbol{\gamma}) = \frac{\Delta M_{e,i}(\boldsymbol{\gamma})}{\Delta \tilde{M}_{e,max}}$$

where \bar{P}_i , $\Delta \bar{M}_{f,i}$ and $\Delta \bar{M}_{e,i}$ are respectively the normalized power and the maximum variation in the flapwise and edgewise bending moments of turbine i . The tuning parameter of the optimization objective is λ , where $\lambda = 1$ corresponds to a single-objective optimization of the power production and $\lambda = 0$ of the loads. Any intermediary values would define a multi-objective optimization. Finally, \tilde{P}_{max} , $\Delta \tilde{M}_{f,max}$ and $\Delta \tilde{M}_{e,max}$ are respectively the estimations of the maximum possible values of the power, differential flapwise bending moment and differential edgewise bending moment of a turbine at a certain wind speed which are obtained through a series of simulations (see Section 4-1). This method ensures that power and loads are balanced (i.e. for $\lambda = 0.5$, power and loads are weighted equally).

3-4-2 Game-theoretic optimization

For the optimization results of a 2-turbine setup (Section 4-2) a game-theoretic approach was utilized. The game-theoretic approach works by making random perturbations to the yaw settings and using these as the new baseline if they yield an improvement over the previous baseline. Using this approach, the global minimum is iteratively approximated.

The decision for this algorithm was based on the discovery of many local minimums in the objective function which are caused by the discrete nature of the velocities in the different wake zones. As the game-theoretic optimization approximates the global optimum, it's not very sensitive to local minimums. The downside of the game-theoretic approach is that, depending on the size of the search space, a significant amount of function evaluations might be required. Fortunately, the computational framework consisting of a 2-turbine setup only takes 0.76 seconds to evaluate on a 3.30 Ghz machine. Also, the problem only has 2 unknown yaw-settings. Therefore, computational feasibility is not a problem.

The game-theoretic algorithm is applied similar to Gebraad et al. [2014a] and can be seen in Algorithm 1. In the lines 1 – 5 the algorithm is initialized and the set of discretized yaw-settings $\boldsymbol{\gamma}$ are given initial values. The remainder of the code is looped till a number of iterations K_{max} is executed. In line 8 the value of the cost-function $c(\boldsymbol{\gamma})$ is updated using the yaw-settings. In the lines 9 – 12 the updated cost-function and yaw-settings are set as the baseline cost \bar{c} and yaw-settings $\bar{\boldsymbol{\gamma}}$ if they yield an improvement over the previous baseline. Finally, in the lines 13 – 20 the yaw-settings for the next iteration are chosen randomly from the set of available yaw-settings based on a uniform distribution

$\mathcal{D}(\gamma_{min}, \gamma_{max})$. The exploration factor E_e is used to determine the likelihood that the algorithm chooses a new yaw-setting and doesn't keep the previous one.

Algorithm 1 The pseudocode below demonstrates how the set of optimal yaw-settings γ is found, similar to Gebraad et al. [2014a]. The maximum number of iterations is K_{max} and \mathcal{D} indicates an uniform distribution. The cost-function $c(\gamma)$ is described in Equation 3-17 where γ_{min} and γ_{max} are the constraints on the search space. E_e Is the exploration factor.

```

1:  $\gamma_i \leftarrow 0 \forall i \in \mathcal{U}$ 
2:  $k \leftarrow 0$ 
3: update  $c(\gamma)$ 
4:  $\bar{c} \leftarrow c(\gamma)$ 
5:  $\bar{\gamma}_i = \gamma_i \forall i \in \mathcal{U}$ 
6: while  $k \leq K_{max}$  do
7:    $k \leftarrow k + 1$ 
8:   update  $c(\gamma)$ 
9:   if  $c(\gamma) > \bar{c}$  then
10:     $\bar{\gamma}_i \leftarrow \gamma_i \forall i \in \mathcal{U}$ 
11:     $\bar{c} \leftarrow c(\gamma)$ 
12:   end if
13:   for  $i \in \mathcal{U}$  do
14:      $R_1 \leftarrow$  random value  $\sim \mathcal{D}(0, 1)$ 
15:     if  $R_1 < E_e$  then
16:        $\gamma_i \leftarrow \mathcal{D}(\gamma_{min}, \gamma_{max})$ 
17:     else
18:        $\gamma_i \leftarrow \bar{\gamma}_i$ 
19:     end if
20:   end for
21: end while

```

3-4-3 Gradient-based optimization

For the simulation results presented in Section 4-3, a gradient-based algorithm was used. The decision for this algorithm was motivated by the fact that an evaluation of the model of a 9-turbine setup takes 9.8s on a 3.30 GHz machine. The search space of 9 yaw-settings is sufficiently large to render any global optimization approach unfeasible with the computational resources available for this work. Therefore, the necessity for a more efficient optimization approach arises.

Gradient-based optimization algorithms are susceptible to local minimums. The discrete wake zones that FLORIS maintains cause local minimums to occur in the search space. Smoothing out the wake zones by fitting a curve removes this problem (Section 3-1-1). To further speed up the optimization procedure, the algorithm was adapted for

multi-threading using *mpi4py* Dalcín et al. [2008].

A limited-memory Broyden-Fletcher-Goldfarb-Shanno (BFGS) algorithm is used to optimize the yaw settings Avriel [2003]. This quasi-Newton algorithm uses an approximation of the inverse Hessian to steer its search through the design space. Note that the search space is not guaranteed to be convex, so this method doesn't guarantee finding the global optimum.

Chapter 4

Simulation results

In this section, the results of three simulation scenarios are presented. In the first scenario, a downstream turbine is swept through the wake of an upstream turbine in order to study the effects of partial wake overlap on the power and the loads. The second scenario will consist of various cases in which the yaw settings of an array of 2 turbines are optimized using a GT-approach. The final scenario performs a mixed-objective optimization of power and loads of a 3x3 wind farm in all wind directions using a gradient-based optimization approach. All simulations are done assuming a constant wind velocity of $U_\infty = 8$ m/s, air viscosity $\mu = 1.81206e^{-5}$ m³/s and air density $\rho = 1.225$ kg/m³. Only the final simulation utilizes smoothing of the velocity distribution, as described in Section 3-1-1.

4-1 The Effect of Partial Wake Overlap on Power Production and Loads

The first simulation setup consists of an array of two wind turbines (Figure 4-1), spaced 6 rotor diameters apart in the x direction while both turbines are yawed into the wind ($\gamma = 0$). The effects of partial wake overlap are investigated by sweeping turbine 2 through the wake of turbine 1 in the y -direction. The distance from the center of turbine 1 to the y -coordinate of turbine 2 is indicated by dY . The results of this simulation are used to obtain the maximum values \tilde{P}_{max} , $\tilde{M}_{f,max}$ and $\tilde{M}_{e,max}$ in the cost functional (Equation 3-17).

The results are shown in Figure 4-2. It can be seen that partial wake overlap results in a significant increase in the loads, which is unfavorable. Furthermore, the loading and power production are not completely symmetric over the range of dY . The maximum

loading is higher when the center of turbine 2 is above the wake center. This is likely caused by the effect of the rotational direction of the rotor blade on the wake. Furthermore, several degrees of wake overlap differently affect the power production and the loads. Full symmetric wake overlap ($dY=0$ m) results in close-to-minimum loading but also sub-optimal power production. Partial wake overlap (i.e. $dY=80$ m) comes with an increased power production, but also significantly increases the loads. Finally, no wake overlap (i.e. $dY=170$ m) maximizes both the power and minimizes the loads. In the situation where $dY=0$, these optima might not be feasible by just yawing turbine 1 as the maximum amount of wake deflection through yawing is limited. This forms motivation for the claim that the potential load reduction while increasing the power production for a given wind farm layout will strongly depend on the wind direction. This problem is further addressed in the next section.

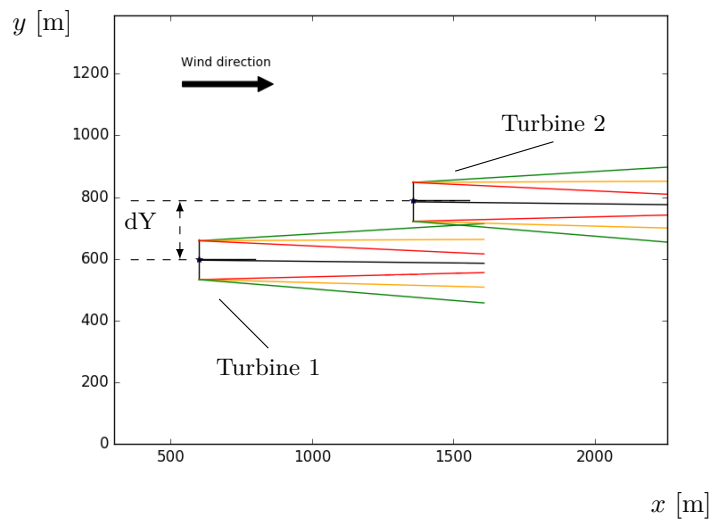


Figure 4-1: Lay-out consisting of 2 turbines with an incoming wind velocity of $U_\infty = 8$ m/s. Turbine 2 is swept through the wake of turbine 1

4-2 Optimization of the Power and the Loads for a 2-turbine case

In this section, the optimization results are presented for an array of two turbines which corresponds to Figure 4-1 for $dY=0$. The optimization is performed using a mixed-objective cost-function (Equation 3-17) for the wind directions $\Phi \in \{0^\circ, 5^\circ, 10^\circ\}$. The results are obtained using the game-theoretic optimization approach (Section 3-4-2). Through experiments it was determined that $K_{max} = 4000$ iterations were sufficient for the algorithm to closely approximate the global maximum with an exploration factor $E_e = 0.4$. For each wind direction, the following cases will be considered:

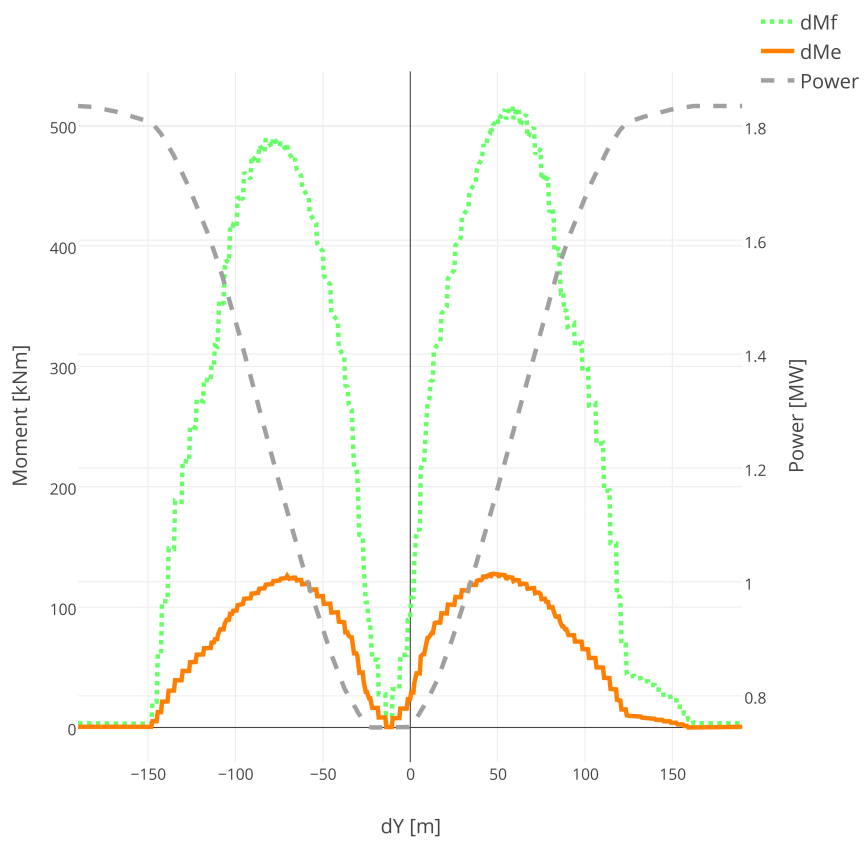


Figure 4-2: The total power production (P), differential flapwise moment (ΔM_f) and edgewise moment (ΔM_e) of turbine 2 versus dY

- Baseline: The yaw-settings are chosen such that both turbines maximize their individual power production. These settings are referred to as *greedy*.
- Case 1 ($\lambda=1$): Single-objective optimization of the power.
- Case 2 ($\lambda=0.97$): Multi-objective optimization of both the power and the loads.
- Case 3 ($\lambda=0.90$): Similar to Case 2, with a stronger emphasis on the loads.
- Case 4 ($\lambda=0$): Single-objective optimization of the loads.

The results are presented in Table 4-1. The optimized yaw settings are shown in Table 4-2. A trend can be seen in each case over all wind directions. An optimization of the power ($\lambda = 1$) will steer the wake of turbine 1 away from the downstream turbine, striving for zero wake overlap. The optimizer also yaws the downstream turbine to accommodate for rotational effects in the wake. The minimization of the loads ($\lambda = 0$) will set the yaw of turbine 1 so that the wake is evenly distributed over the rotor disk of the downstream turbine, or if possible, is avoided all together. The combined optimizations ($\lambda = 0.97$ and $\lambda = 0.90$) find a trade-off between the two objectives.

In general, optimizing the power production through yaw-misalignment heavily increases the loads for $\Phi = 0$, and decreases the loads for $\Phi = 5^\circ$ and $\Phi = 10^\circ$. In the case of $\Phi = 0^\circ$, there is only a small reduction in loads possible without heavily penalizing the power production. For $\Phi = 5^\circ$ and $\Phi = 10^\circ$, Case 1-3 will result in both an increase in power, and a great reduction in loading compared to the baseline. This has to do with the fact that partial wake overlap was already present before the optimization. Case 2 and 3 are able to achieve additional reductions in loading opposed to Case 1 at the expense of a small amount of power production.

The Pareto fronts of the cumulative power and differential loading for various wind directions are depicted in Figure 4-3. It can be seen that for $\Phi = 0^\circ$, increasing the power comes with an inevitable increase of differential loading. For $\Phi = 5^\circ$ and $\Phi = 10^\circ$, more of a trade-off can be made between power and loading. The use of a mixed-objective optimization is most beneficial for $\Phi = 10^\circ$, as a significant loading decrease can be obtained at the expense of a small amount of power production.

4-3 Optimization of the Power and the Loads for a wind farm

This section presents the results of a omnidirectional optimization of a wind farm. A wind farm consisting of 3 arrays of 3 wind turbines is optimized in all wind directions $\Phi \in \{0^\circ, 5^\circ, \dots, 355^\circ\}$. The resulting power productions and loadings are averaged over all wind directions and presented. The optimization is performed using a mixed-objective cost-function (Equation 3-17) and the following cases will be considered:

- Baseline: The yaw-settings are chosen such that both turbines maximize their individual power production. These settings are referred to as *greedy*.

Table 4-1: Optimization results for various cost functions and wind directions of a 2-turbine array. The results are expressed in % change compared to the baseline case

Φ		P_{tot}	$\sum \Delta M_f$	$\sum \Delta M_e$
0°	$\lambda = 1$	3.75	342.71	352.89
	$\lambda = 0.97$	3.58	304.53	313.06
	$\lambda = 0.90$	-1.02	-93.99	-96.17
	$\lambda = 0$	-18.69	-95.35	-96.76
5°	$\lambda = 1$	5.49	-5.14	163.90
	$\lambda = 0.97$	5.39	-10.07	150.97
	$\lambda = 0.90$	5.39	-10.07	150.97
	$\lambda = 0$	-53.01	-93.21	-84.20
10°	$\lambda = 1$	0.98	-66.35	-93.01
	$\lambda = 0.97$	0.92	-86.98	-96.95
	$\lambda = 0.90$	0.68	-95.59	-99.38
	$\lambda = 0$	-57.85	-98.45	-99.67

Table 4-2: Resulting yaw settings of the various optimizations

	Baseline		Case 1 ($\lambda = 1$)		Case 2 ($\lambda = 0.97$)		Case 3 ($\lambda = 0.90$)		Case 4 ($\lambda = 0$)	
	γ_1	γ_2	γ_1	γ_2	γ_1	γ_2	γ_1	γ_2	γ_1	γ_2
$\Phi = 0^\circ$	0°	0°	15.5°	0.3°	15.2°	0.3°	-4.9°	0.3°	-6.8°	-40°
$\Phi = 5^\circ$	0°	0°	-13.6°	0.4°	-15.2°	0.3°	-15.2°	0.3°	39.9°	-39.9°
$\Phi = 10^\circ$	0°	0°	-5.2°	0.3°	-6.5°	0.4°	-7.9°	0.3°	-40°	-40°

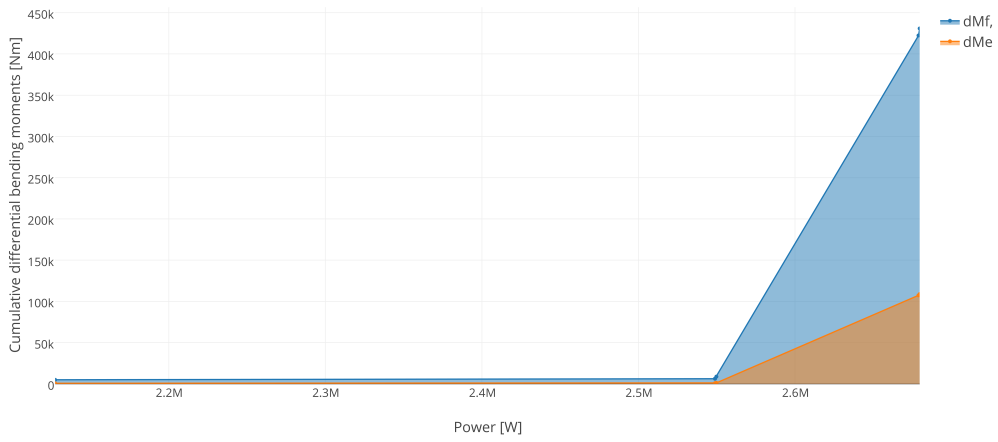
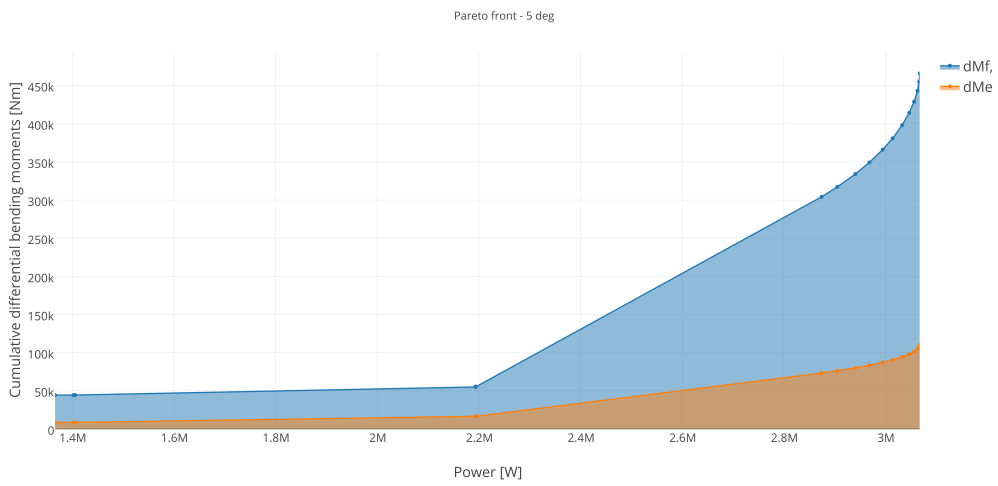
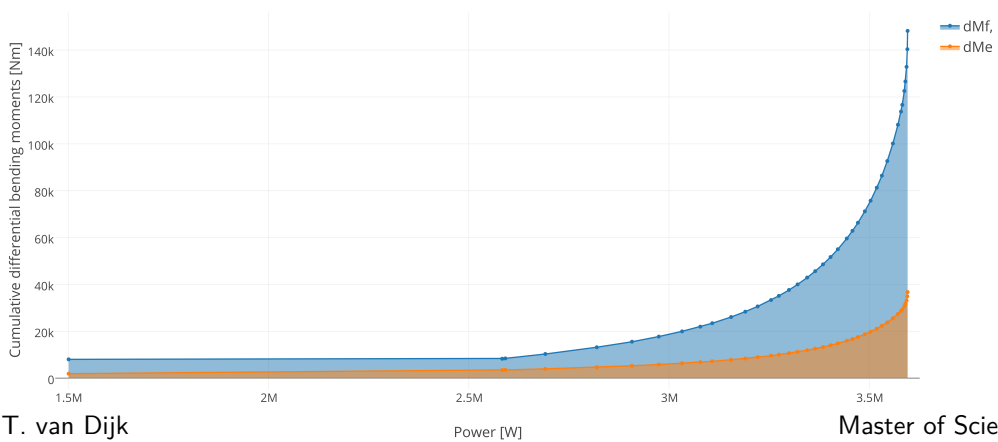
(a) Wind direction of 0° (b) Wind direction of 5° (c) Wind direction of 10°

Figure 4-3: Pareto fronts of total power and cumulative differential loading for various wind directions

- Case 1 ($\lambda = 1$): Single-objective optimization of the power.
- Case 2 ($0 < \lambda < 1$): Multi-objective optimization of both the power and the loads.
- Case 3 ($\lambda = 0$): Single-objective optimization of the loads.

In Figure 4-4 and 4-5, the yaw-settings of a power-only optimization and a combined optimization are compared. As the figure shows, the power optimization yawed the first column of turbines to increase the power production of the second column. The combined optimization did not, as that would have significantly increased the differential loads. Nonetheless, the power production due to the optimized settings is still higher than the baseline.

The results of the single-objective optimization of the power ($\lambda = 1$) are presented in Figure 4-6a, 4-6c and 4-6e. It can be seen that for most of the wind directions, a gain in power production can be obtained over the baseline. The differential flap and edgewise loads decrease in wind directions where partial wake overlap was already present in the baseline case. Situations where symmetrical wake overlap occurred in the baseline case show significantly increased differential loads of up to 200% of the baseline when optimized. This reveals a necessity for a trade-off between potential power gain and change of differential loads.

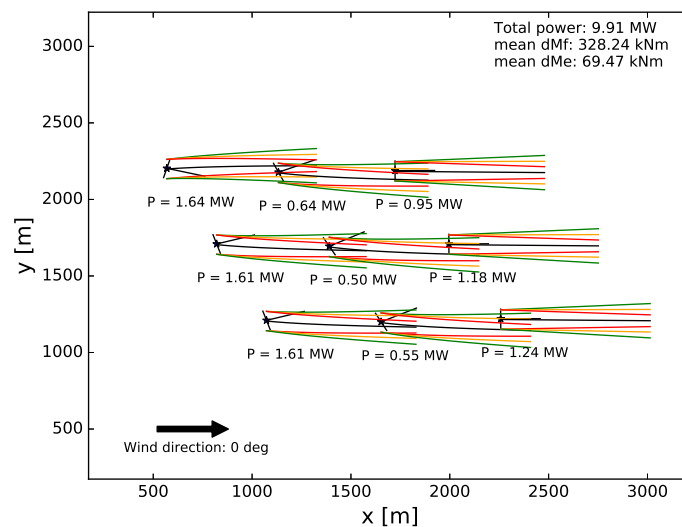


Figure 4-4: Single-objective optimization of the power ($\lambda = 1.0$) for $\Phi = 0^\circ$. As a reference, the baseline power is $\sum_{i=1}^9 P_i = 8.92$ MW, and the mean differential flapwise and edgewise moments are respectively 168.03 kNm and 43.67 kNm

The results of the combined-objective optimization ($\lambda = 0.8$) are presented in Figure 4-6b, 4-6d and 4-6f. Compared to the single-objective optimization, it can be seen that

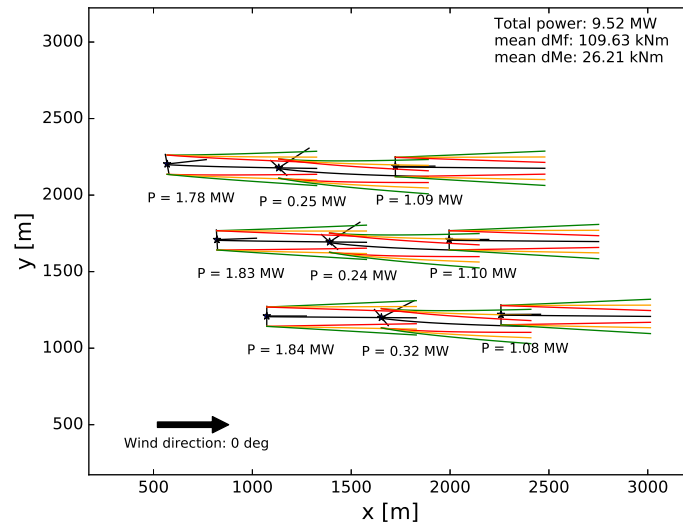


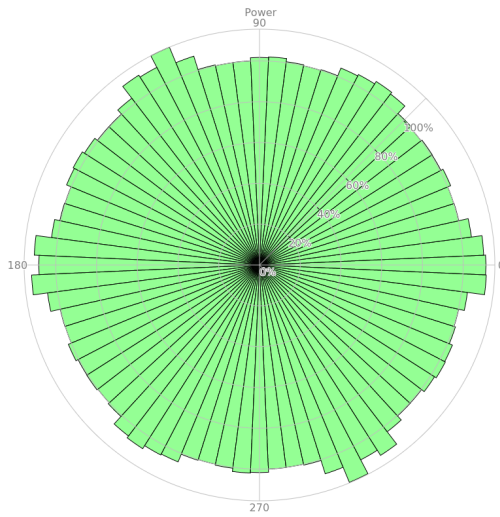
Figure 4-5: Multi-objective optimization of power and loads ($\lambda = 0.8$) for $\Phi = 0^\circ$. As a reference, the baseline power is $\sum_{i=1}^9 P_i = 8.92$ MW, and the mean differential flapwise and edgewise moments are respectively 168.03 kNm and 43.67 kNm.

the magnitude of the optimized power has slightly reduced in most wind directions. On the other hand loads at $\Phi = 0^\circ$ and $\Phi = 120^\circ$ have also decreased as the optimizer sacrificed power production to decrease the loading.

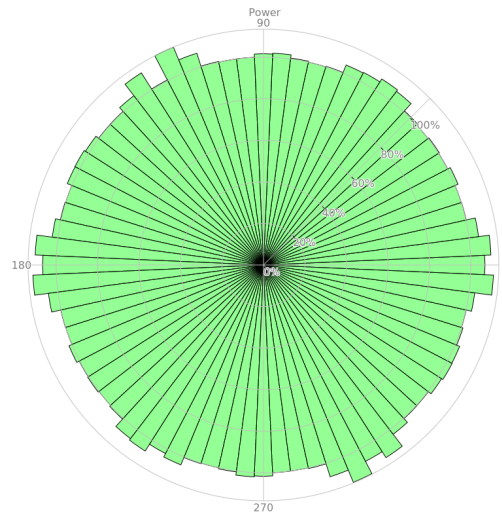
Several optimization strategies with different weights for loads and power are presented in Figure 4-7 and in Table 4-3. For each wind direction, the total power production, mean differential flapwise and edgewise bending moments are measured (Section 3-4). The results are averaged over all wind directions to obtain the final results. It can be seen that both the power optimization $\lambda = 1$ and combined optimizations $\lambda = \{0.9, 0.8, 0.7\}$ result in increased power production over the baseline and reduced mean loading in the wind farm.

A loads-only optimization reveals the greatest reduction in loading that can be achieved, but suffers from reduced power production and is therefore not desirable. The mixed-objective optimization sacrifices some power production for a much larger decrease of the average differential loading of the wind farm. The mixed-objective optimization with $\lambda = 0.7$ produces similar mean power as the baseline, but comes with a load reduction of 40 – 45%. This suggests that yaw-misalignment could be used as a method to reduce fatigue loading due to partial wake overlap.

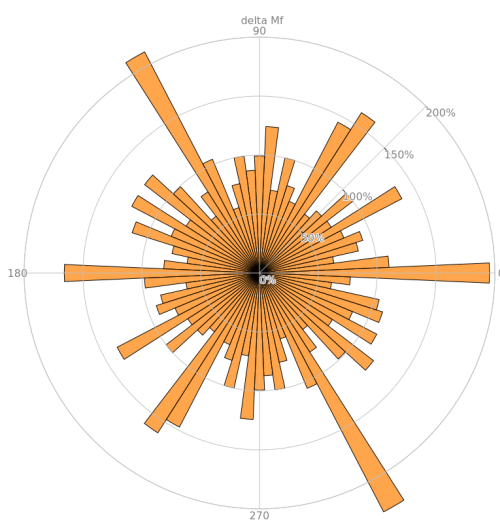
A combined optimization for a single wind direction took on average 216 s on a 3.4 GHz 8-core system. The total simulation time for one tuning parameter in all wind directions was 4.3 hours.



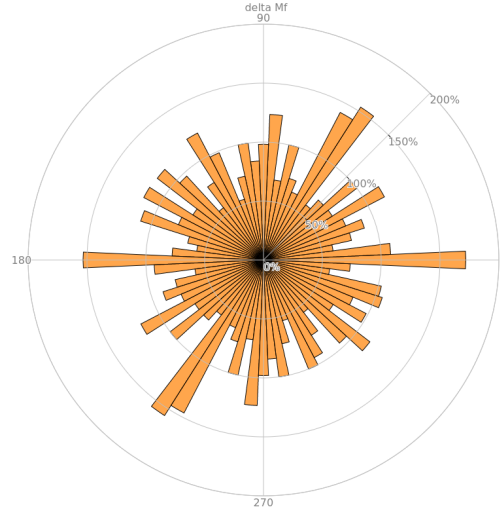
(a) Optimized power for various wind directions ($\lambda = 1.0$)



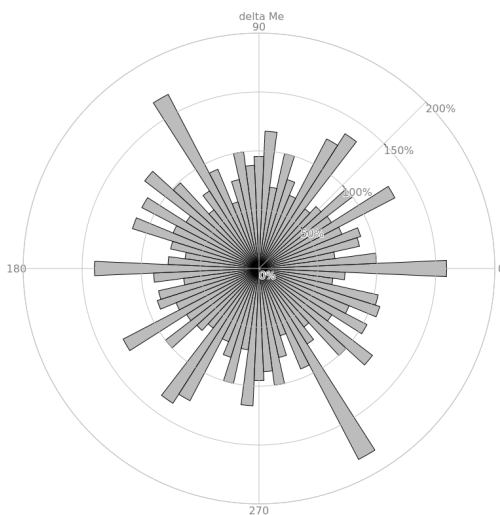
(b) Optimized power for various wind directions ($\lambda = 0.8$)



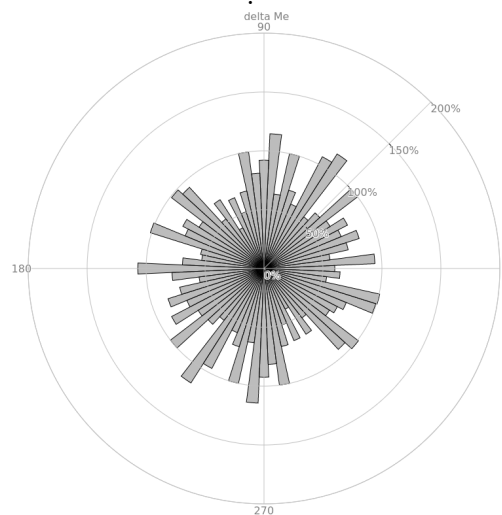
(c) Optimized ΔMf for various wind directions ($\lambda = 1.0$)



(d) Optimized ΔMf for various wind directions ($\lambda = 0.8$)



(e) Optimized ΔMe for various wind directions ($\lambda = 1.0$)



(f) Optimized ΔMe for various wind directions ($\lambda = 0.8$)

Figure 4-6: Simulation results for the full spectrum of wind directions. All results are expressed as part of the baseline.

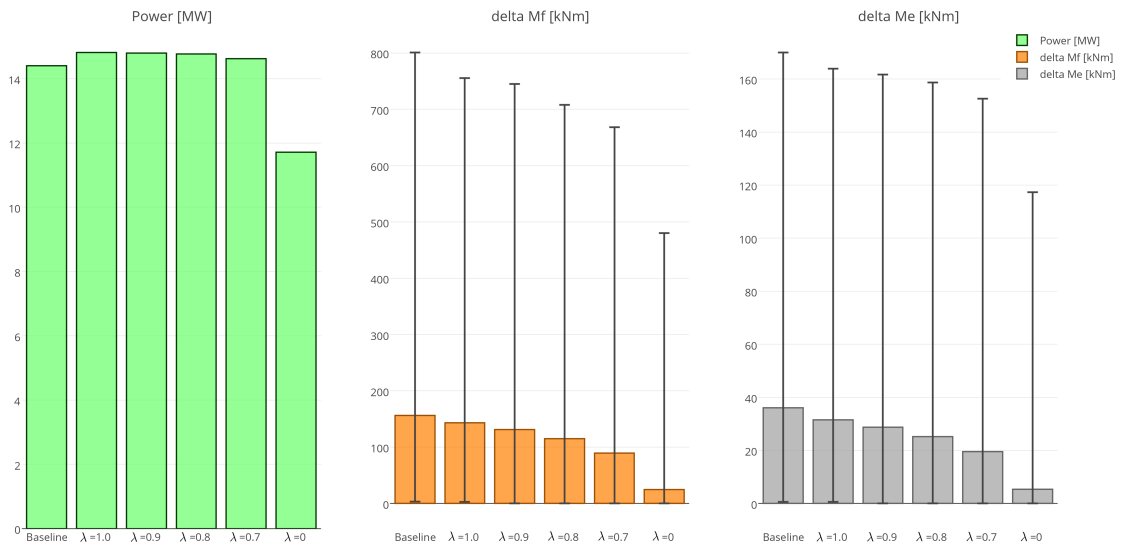


Figure 4-7: Comparison of respectively the mean total wind farm power P , mean differential flapwise ΔM_f and edgewise ΔM_e loading for all wind directions Φ . The maximum and minimum turbine loading for any wind direction that occurred in the wind farm are indicated. The tuning parameter 'C' is used analogous to λ .

Table 4-3: Comparison of respectively the mean total wind farm power P , mean differential flapwise ΔM_f and edgewise ΔM_e loading for all wind directions Φ . Results are expressed in % change to the baseline.

	mean P	mean ΔM_f	mean ΔM_e
$\lambda = 1$	2.85%	-8.17%	-12.48%
$\lambda = 0.9$	2.74%	-15.75%	-20.10%
$\lambda = 0.8$	2.49%	-26.12%	-30.12%
$\lambda = 0.7$	1.53%	-42.67%	-45.70%
$\lambda = 0$	-18.72%	-84.21%	-85.04%

Conclusion, Discussion and Recommendations

5-1 Conclusion and Discussion

This thesis aims to quantify the load variations due to partial wake overlap and investigates the effect thereof on the optimal yaw settings. Furthermore, the benefits are evaluated of including differential loads in a wind farm power optimization using yaw misalignment. The optimization is multi-objective in that it maximizes the power production while taking into account the load variations. The power production and loads were computed using an optimization framework that modeled yaw misalignment, wake interaction and partial wake overlap for multi-turbine setups.

The results of the first simulation show that partial wake-overlap greatly increases the differential flapwise and edgewise bending moments compared to full symmetrical wake overlap. The results suggest that in cases where greedy settings would result in full wake overlap, power optimization by yaw misalignment might not be desirable. This depends on whether the wake can be redirected as to avoid the downstream turbine, because partial wake overlap might cause the differential blade loading to increase significantly.

Various simulation cases of a 2-turbine setup for several wind directions confirmed this. It was shown that optimizing for power will result in a significant increase in differential rotor loading in situations where greedy settings would result in full symmetric wake overlap. A decline was observed when the optimal yaw settings were able to greatly decrease the wake overlap. The optimal yaw settings resulted in an increase in loading of up to 350% for $\Phi = 0$ but in a decrease for $\Phi = 5$ and $\Phi = 10$. This suggests that yaw misalignment is a desirable method to increase the power in situations where the

wake can be sufficiently directed away from the downstream turbine, as this positively affects the rotor fatigue loads.

Finally, a mixed-objective power and loads optimization was performed on a wind farm in all wind directions. A power only optimization was found to increase the mean total omnidirectional power by 4% compared to the greedy settings and decrease the mean differential flap and edgewise loads by respectively 19% and 21%. The mixed-objective optimization found an omnidirectional power production of 1.9% and a mean differential flap and edgewise loading decrease of respectively 41% and 50% compared to greedy settings. This shows that yaw-misalignment can be beneficial to both increase the power and decrease differential loading due to partial wake overlap if the optimization algorithm takes into account the topology and the loading.

This work presents preliminary results of mixed-objective wind farm optimization using yaw misalignment and is bound to a number of limitations. The optimization framework used for this thesis utilizes steady-state models for the purpose of computational efficiency. The use of dynamic models could increase the understanding of how partial wake overlap affects wind turbine loading. Phenomena such as turbulence and the transition from full to partial wake overlap could be investigated. Furthermore, individual pitch control might be able to mitigate a portion of the loading caused by partial wake overlap.

The optimization utilizes the same tuning parameter λ (Equation 3-17) in every wind direction while the shape of the cost-function might change. Since the parameter isn't tuned for every individual wind direction, the presented results might not be optimal. Also, for the final simulation results the power and load results are averaged over all wind directions, instead of using a realistic wind spectrum. Doing so might provide different results. Furthermore, the cost function is not convex and therefore the results are not guaranteed to be optimal. Nonetheless, they are a notable improvement over the baseline.

5-2 Recommendations

This work presents preliminary results and further research is required to provide conclusive evidence on the benefits of mixed-objective wind farm optimization using yaw-misalignment. First of all, the use of dynamic models could increase the understanding of how partial wake overlap affects wind turbine loading. Phenomena such as turbulence and the transition from full to partial wake overlap could be investigated.

The implementation of a dynamic model would also allow more sophisticated techniques for computing fatigue loads, such as Rainflow counting Downing and Socie [1982]. This would necessitate increasing the computational efficiency of the model or access to more powerful computational resources to keep the optimization time feasible. To verify that the optimized yaw settings will indeed decrease the rotor fatigue loading while increasing the power, a validation using high fidelity models and realistic wind data is required.

Including other loads such as the flapwise bending moment, edgewise bending moment, drivetrain torsion and tower bending moment in the cost function might provide different optimal yaw settings. Also, the effect of wind shear is interesting to include as it has been shown to affect the wind turbine fatigue Eggers et al. [2003].

Individual pitch control might be able to mitigate a portion of the rotor loads caused by partial wake overlap. Therefore, it is recommended to evaluate the fatigue loading due to partial wake overlap on a turbine with active individual pitch control.

Finally, it would be interesting to develop an online controller that simultaneously maximizes the power while mitigating the differential loads. A candidate model would be FloriDyn Gebraad et al. [2015], a modified version of FLORIS with a delay model. The computational efficiency of FloriDyn would allow for online optimization, and results can be validated with high-fidelity simulation data. This would yet bring the state-of-the-art one step closer to online optimization of power and loads of a real wind farm.

Bibliography

- Jennifer Annoni, Pieter MO Gebraad, Andrew K Scholbrock, Paul A Fleming, and Jan-Willem van Wingerden. Analysis of axial-induction-based wind plant control using an engineering and a high-order wind plant model. *Wind Energy*, 2015.
- Turaj Ashuri. *Beyond classical upscaling: Integrated aeroservoelastic design and optimization of large offshore wind turbines*. PhD thesis, Delft University of Technology, The Netherlands, 2012.
- Turaj Ashuri and MB Zaaijer. Size effect on wind turbine blade's design drivers. In *European Wind Energy Conference and exhibition, Brussels, Belgium*, pages 1–6. European Wind Energy Association, 2008.
- Turaj Ashuri and Michiel B Zaaijer. Review of design concepts, methods and considerations of offshore wind turbines. In *European Offshore Wind Conference and Exhibition, Berlin, Germany*, pages 1–10. European Wind Energy Association, 2007.
- Turaj Ashuri, Gerard JW Van Bussel, Michiel B Zaaijer, and Gijs AM Van Kuik. Controller design automation for aeroservoelastic design optimization of wind turbines. In *The Science of making Torque from Wind, Heraklion, Crete, Greece*, pages 1–7. European Wind Energy Association, 2010.
- Turaj Ashuri, Gerard Bussel, and Stefan Mieras. Development and validation of a computational model for design analysis of a novel marine turbine. *Wind Energy*, 16(1):77–90, 2013.
- Turaj Ashuri, Michiel B Zaaijer, Joaquim RRA Martins, Gerard JW van Bussel, and Gijs AM van Kuik. Multidisciplinary design optimization of offshore wind turbines for minimum levelized cost of energy. *Renewable Energy*, 68(0):893–905, 2014.

- Turaj Ashuri, Mario Rotea, Yan Xiao, Yaoyu Li, and Chandra Verma Ponnurangam. Wind turbine performance decline and its mitigation via extremum seeking controls. In *AIAA Science and Technology Forum and Exposition (SciTech), Wind Energy Symposium, San Diego, California*, pages 1–11. AIAA, 2016a.
- Turaj Ashuri, Tao Zhang, Dong Qian, and Mario Rotea. Uncertainty quantification of the levelized cost of energy for the 20MW research wind turbine model. In *AIAA Science and Technology Forum and Exposition (SciTech), Wind Energy Symposium, San Diego, California*, page 1998. AIAA, 2016b.
- Mordecai Avriel. *Nonlinear programming: analysis and methods*. Courier Corporation, 2003.
- A Behnood, Hamid Gharavi, B Vahidi, and GH Riahy. Optimal output power of not properly designed wind farms, considering wake effects. *International Journal of Electrical Power & Energy Systems*, 63:44–50, 2014.
- Fernando D Bianchi, Hernan De Battista, and Ricardo J Mantz. *Wind turbine control systems: principles, modelling and gain scheduling design*. Springer Science & Business Media, 2006.
- María Isabel Blanco. The economics of wind energy. *Renewable and Sustainable Energy Reviews*, 13(6):1372–1382, 2009.
- Mark Bolinger and Ryan Wiser. Wind power price trends in the united states: struggling to remain competitive in the face of strong growth. *Energy Policy*, 37(3):1061–1071, 2009.
- Koen Boorsma. Power and loads for wind turbines in yawed conditions. Technical report, ECN-E-12-047, ECN, Petten, The Netherlands, 2012.
- Arno J Brand. Aeolus deliverable 1.3. preliminary maps of wind fields and mechanical loads and energy. Technical report, Technical report, Energy research Centre of The Netherlands, 2009.
- Pablo Castillo Capponi, Turaj Ashuri, Gerard JW van Bussel, and Bjarne Kallesøe. A non-linear upscaling approach for wind turbine blades based on stresses. In *European Wind Energy Conference and Exhibition, Brussels, Belgium*, pages 1–8. The European Wind Energy Association, 2011.
- Matt Churchfield, Paul Fleming, Bernard Bulder, and Stanley M. White. Wind turbine wake-redirection control at the fishermen’s atlantic city windfarm: Preprint. Technical report, NREL (National Renewable Energy Laboratory (NREL), Golden, CO (United States)), 2015.
- Matthew Churchfield, John Michalakes, Philippe Spalart, and Patrick Moriarty. High-fidelity simulation comparison of wake mitigation control strategies for a two-turbine case. *Wind Energy*, 18(12):2135–2143, 2014.

- Gustav P Corten and Pieter Schaak. Heat and flux: Increase of wind farm production by reduction of the axial induction. In *Proceedings of the European Wind Energy Conference*, 2003.
- Lisandro Dalcín, Rodrigo Paz, Mario Storti, and Jorge D'Elía. Mpi for python: Performance improvements and mpi-2 extensions. *Journal of Parallel and Distributed Computing*, 68(5):655–662, 2008.
- Eleanor Denny. The economics of tidal energy. *Energy Policy*, 37(5):1914–1924, 2009.
- Stephen D Downing and DF Socie. Simple rainflow counting algorithms. *International journal of fatigue*, 4(1):31–40, 1982.
- Erika Echavarria, Berthold Hahn, Gerard J van Bussel, and Tetsuo Tomiyama. Reliability of wind turbine technology through time. *Journal of Solar Energy Engineering*, 130(3), 2008.
- Ottmar Edenhofer, Ramón Pichs-Madruga, and Youba Sokona. Mitigation of climate change. *Climate Change*, pages 6–9, 2014.
- Alfred J Eggers, Ramarao Digumarthi, and Keith Chaney. Wind shear and turbulence effects on rotor fatigue and loads control. In *ASME 2003 Wind Energy Symposium*, pages 225–234. American Society of Mechanical Engineers, 2003.
- Paul Fleming, Pieter MO Gebraad, Jan-Willem van Wingerden, Sang Lee, Matt Churchfield, Andrew Scholbrock, John Michalakes, Kathryn Johnson, and Pat Moriarty. The SOWFA super-controller: A high-fidelity tool for evaluating wind plant control approaches. In *EWEA Annual Meeting, Vienna, Austria*, 2013.
- Paul Fleming, Pieter MO Gebraad, Sang Lee, Jan-Willem Wingerden, Kathryn Johnson, Matt Churchfield, John Michalakes, Philippe Spalart, and Patrick Moriarty. Simulation comparison of wake mitigation control strategies for a two-turbine case. *Wind Energy*, 18(12):2135–2143, 2015a.
- Paul A Fleming, Pieter MO Gebraad, Sang Lee, Jan-Willem van Wingerden, Kathryn Johnson, Matt Churchfield, John Michalakes, Philippe Spalart, and Patrick Moriarty. Evaluating techniques for redirecting turbine wakes using SOWFA. *Renewable Energy*, 70:211–218, 2014.
- Paul A Fleming, Andrew Ning, Pieter MO Gebraad, and Katherine Dykes. Wind plant system engineering through optimization of layout and yaw control. *Wind Energy*, 2015b.
- Sten Frandsen, Rebecca Barthelmie, Sara Pryor, Ole Rathmann, Søren Larsen, Jørgen Højstrup, and Morten Thøgersen. Analytical modelling of wind speed deficit in large offshore wind farms. *Wind energy*, 9(1-2):39–53, 2006.

- Vasilis Fthenakis and Hyung Chul Kim. Land use and electricity generation: A life-cycle analysis. *Renewable and Sustainable Energy Reviews*, 13(6):1465–1474, 2009.
- Pieter MO Gebraad and Jan-Willem van Wingerden. Maximum power-point tracking control for wind farms. *Wind Energy*, 18(3):429–447, 2015.
- Pieter MO Gebraad, Filip C van Dam, and Jan-Willem van Wingerden. A model-free distributed approach for wind plant control. In *American Control Conference (ACC), 2013*, pages 628–633. IEEE, 2013.
- Pieter MO Gebraad, Floris W Teeuwisse, Jan-Willem van Wingerden, Paul A Fleming, Shalom D Ruben, Jason R Marden, and Lucy Y Pao. A data-driven model for wind plant power optimization by yaw control. In *American Control Conference (ACC), 2014*, pages 3128–3134. IEEE, 2014a.
- Pieter MO Gebraad, Floris W Teeuwisse, Jan-Willem Wingerden, Paul A Fleming, Shalom D Ruben, Jason R Marden, and Lucy Y Pao. Wind plant power optimization through yaw control using a parametric model for wake effects—a cfd simulation study. *Wind Energy*, 2014b.
- Pieter MO Gebraad, Paul A Fleming, and Jan-Willem van Wingerden. Wind turbine wake estimation and control using flordyn, a control-oriented dynamic wind plant model. In *2015 American Control Conference (ACC)*, pages 1702–1708. IEEE, 2015.
- Jay P Goit and Johan Meyers. Optimal control of energy extraction in wind-farm boundary layers. *Journal of Fluid Mechanics*, 768:5–50, 2015.
- Flavio Heer, Peyman Mohajerin Esfahani, Maryam Kamgarpour, and John Lygeros. Model based power optimisation of wind farms. In *Control Conference (ECC), 2014 European*, pages 1145–1150. IEEE, 2014.
- Jürgen Herp, Uffe V Poulsen, and Martin Greiner. Wind farm power optimization including flow variability. *Renewable Energy*, 81:173–181, 2015.
- Tomislav Horvat, Vedrana Spudić, and Mato Baotić. Quasi-stationary optimal control for wind farm with closely spaced turbines. In *MIPRO, 2012 Proceedings of the 35th International Convention*, pages 829–834. IEEE, 2012.
- Peter Jamieson. *Innovation in wind turbine design*. John Wiley & Sons, 2011.
- NO Jensen. A note on wind turbine interaction. *Risoe National Laboratory, Roskilde, Denmark, Technical Report No. M-2411*, 1983.
- Ángel Jiménez, Antonio Crespo, and Emilio Migoya. Application of a les technique to characterize the wake deflection of a wind turbine in yaw. *Wind energy*, 13(6):559–572, 2010.
- Jason Mark Jonkman, Sandy Butterfield, Walter Musial, and George Scott. Definition of a 5-mw reference wind turbine for offshore system development, 2009.

- Stoyan K Kanev and Feike J Savenije. Active wake control: loads trends. *Wind Energy*, 2015:2014, 2016.
- I Katic, Jørgen Højstrup, and Niels Otto Jensen. A simple model for cluster efficiency. In *European Wind Energy Association Conference and Exhibition*, pages 407–410, 1986.
- Chunghun Kim, Yonghao Gui, Chung Choo Chung, and Yong-Cheol Kang. A model-free method for wind power plant control with variable wind. In *PES General Meeting/Conference & Exposition, 2014 IEEE*, pages 1–5. IEEE, 2014.
- Torben Knudsen, Thomas Bak, and Mikael Svenstrup. Wind farm control survey. Technical report, 2014.
- Knud A Kragh and Morten H Hansen. Load alleviation of wind turbines by yaw misalignment. *Wind Energy*, 17(7):971–982, 2014.
- Eric Lantz, Ryan Wiser, and Maureen Hand. The past and future cost of wind energy. *National Renewable Energy Laboratory, Golden, CO, Report No. NREL/TP-6A20-53510*, 2012.
- William E Leithead, S De la Salle, and D Reardon. Role and objectives of control for wind turbines. 138(2):135–148, 1991.
- Nathan S Lewis. Toward cost-effective solar energy use. *science*, 315(5813):798–801, 2007.
- Jason R Marden, Shalom D Ruben, and Lucy Y Pao. A model-free approach to wind farm control using game theoretic methods. *Control Systems Technology, IEEE Transactions on*, 21(4):1207–1214, 2013.
- Craig B Markwardt. Non-linear least squares fitting in idl with mpfit. *arXiv preprint arXiv:0902.2850*, 2009.
- Andrew S Ning. *CCBlade Documentation*. 2013.
- S Andrew Ning. A simple solution method for the blade element momentum equations with guaranteed convergence. *Wind Energy*, 17(9):1327–1345, 2014.
- Jinkyoo Park and Kincho H Law. A bayesian optimization approach for wind farm power maximization. In *SPIE Smart Structures and Materials+ Nondestructive Evaluation and Health Monitoring*, pages 943608–943608. International Society for Optics and Photonics, 2015.
- Andrew D Platt and Marshall Buhl. Wt perf user guide for version 3.05. Technical report, 00. Tech. rep., National Renewable Energy Laboratory, Golden, CO, 2012.
- Shu Ching Quek. Systems, devices and methods for improving efficiency of wind power generation systems, 03 2012.

- Mario A Rotea. Dynamic programming framework for wind power maximization. In *Proc. of the 19th IFAC World Congress, Cape Town, South Africa*, pages 3639–3644, 2014.
- Christian Santoni, Umberto Ciri, Mario Rotea, and Stefano Leonardi. Development of a high fidelity cfd code for wind farm control. In *American Control Conference (ACC), 2015*, pages 1715–1720. IEEE, 2015.
- JG Schepers and Sander P Van der Pijl. Improved modelling of wake aerodynamics and assessment of new farm control strategies. 75(1):012039, 2007.
- Jannik Schottler, Agnieszka Hölling, Joachim Peinke, and Michael Hölling. Wind tunnel tests on controllable model wind turbines in yaw. In *34th Wind Energy Symposium*, page 1523, 2016.
- Javier Serrano Gonzalez, Manuel Burgos Payan, and Jesus Riquelme Santos. Optimal control of wind turbines for minimizing overall wake effect losses in offshore wind farms. In *EUROCON, 2013 IEEE*, pages 1129–1134. IEEE, 2013.
- Ralph EH Sims, Hans-Holger Rogner, and Ken Gregory. Carbon emission and mitigation cost comparisons between fossil fuel, nuclear and renewable energy resources for electricity generation. *Energy policy*, 31(13):1315–1326, 2003.
- F Spinato, Peter J Tavner, Gerard JW Van Bussel, and E Koutoulakos. Reliability of wind turbine subassemblies. *Renewable Power Generation, IET*, 3(4):387–401, 2009.
- Christopher John Spruce. *Simulation and control of windfarms*. PhD thesis, University of Oxford, 1993.
- Maarten Steinbuch, WW de Boer, Okko H Bosgra, SAWM Peters, and Jeroen Ploeg. Optimal control of wind power plants. *Journal of Wind Engineering and Industrial Aerodynamics*, 27(1-3):237–246, 1988.
- Patrick Sullivan, Wesley Cole, Nate Blair, Eric Lantz, Venkat Krishnan, Trieu Mai, David Mulcahy, and Gian Porro. 2015 standard scenarios annual report: Us electric sector scenario exploration. Technical report, National Renewable Energy Laboratory (NREL), Golden, CO (United States), 2015.
- Jan-Willem Van Wingerden, Teun Hulskamp, Thanasis Barlas, B Marrant, Gijs AM Van Kuik, DP Molenaar, and Michel Verhaegen. On the proof of concept of a ‘smart’ wind turbine rotor blade for load alleviation. *Wind Energy*, 11(3):265, 2008.
- Zhongzhou Yang, Yaoyu Li, and John E Seem. Maximizing wind farm energy capture via nested-loop extremum seeking control. In *ASME 2013 Dynamic Systems and Control Conference*, pages V003T49A005–V003T49A005. American Society of Mechanical Engineers, 2013.

Glossary

List of Acronyms

